INVESTIGATION OF COMBINED ION EXCHANGE TO DECREASE MEMBRANE FOULING POTENTIAL DURING WATER TREATMENT

By

KATRINA ANNE INDARAWIS

A DISSERTATION PRESENTED TO THE GRADUATE SCHOOL
OF THE UNIVERSITY OF FLORIDA IN PARTIAL FULFILLMENT
OF THE REQUIREMENTS FOR THE DEGREE OF
DOCTOR OF PHILOSOPHY

UNIVERSITY OF FLORIDA

2013

To my God…
for inspiring wonder and excitement to me through the world you created
…that which we call science.

ACKNOWLEDGMENTS

I would first like to thank my husband for all of his patience, love and support. These past four years have been challenging and he has led our family in an amazing way. He put me before himself and sacrificed so much in order for me to achieve my dreams. I absolutely could not have done this without him.

I would also like to thank Dr. Boyer for all of his guidance and support. His contributions to my PhD research are incalculable. I appreciate the push for publications and presentations as it has greatly enhanced my PhD research and subsequently my dissertation. I would especially like to thank Dr. Mazyck for always believing in me. His faith in my ability has allowed me to achieve feats I never thought possible. His recommendation for me as a PhD student has been life-changing and I am forever grateful. I would also like to express my immense gratitude to Dr. Chadik, an anomaly in the academic world. His guidance and support has helped me through important obstacles I have come across in my PhD, both scientifically and emotionally. I would also like to extend a warm thank you to Dr. Zimmerman for his guidance, our talks, and most of importantly for telling me I'm a "good grad student" when I felt like the worst. Those words have helped me believe in myself and make it to the end. Thank you.

I want to thank all the undergraduate students who have volunteered their time in the lab helping me: Troy Chasteen who came in multiple weekends to help filter samples, Weizhi Chang for his dedication and consistent help, Ricky Nayar for staying until 2am to help me filter samples one time, Jeremy Toms for being a huge help to me by coming in nearly every day to help (even when he had exams), and Avni Solanki who

swooped in at the end like an angel and saw my experiments to completion. These guys greatly increased my productivity and I am truly grateful.

TABLE OF CONTENTS

page

LIST OF TABLES

LIST OF FIGURES

LIST OF ABBREVIATIONS

AER	Anion Exchange Resin
CER	Cation Exchange Resin
CIX	Combined Ion Exchange
DOM	Dissolved Organic Matter
NOM	Natural Organic Matter
RO	Reverse Osmosis

Abstract of Dissertation Presented to the Graduate School
of the University of Florida in Partial Fulfillment of the
Requirements for the Degree of Doctor of Philosophy

INVESTIGATION OF COMBINED ION EXCHANGE TO DECREASE MEMBRANE FOULING POTENTIAL DURING WATER TREATMENT

By

Katrina Anne Indarawis

August 2013

Chair: Treavor H. Boyer
Major: Environmental Engineering Sciences

The goal of this research was to determine if combined cation and anion exchange would reduce fouling of reverse osmosis membranes. This research is divided into three parts. The first part provides an improved understanding of the interactions between alkaline earth metals and dissolved organic matter (DOM) under conditions that are encountered during drinking water treatment with particular focus on cation exchange. Both magnetically-enhanced and nonmagnetic cation exchange resins were converted to Na, Mg, Ca, Sr, and Ba mobile counterion forms as a novel approach to investigating the exchange behavior of the cations and the interactions between the cations and DOM. The results show that cation exchange is a robust process for removal of Ca^{2+} and Mg^{2+} considering competition between the cations on the resin surface and presence of DOM. The second part of this research focuses on combined ion exchange and answers the research question, “Can the effects of combined ion exchange be predicted as the sum of anions removed during anion exchange and cations removed during cation exchange?.” Results indicated that combined ion exchange can reduce precipitation of sparingly soluble minerals, such as $CaCO_3$, from the bulk solution by simultaneously removing calcium and bicarbonate. Results showed

that it is possible to estimate sulfate, magnesium, and DOC removal during combined ion exchange by rules of superposition, as well as calcium when the initial concentration of calcium is low. The effect of combined ion exchange on separation factors is also calculated and discussed. The third part of this research compares anion exchange pretreatment, cation exchange pretreatment, and combined ion exchange pretreatment to a natural groundwater before reverse osmosis (RO). This was to determine which ion exchange pretreatment reduced fouling of RO, quantitatively determined by flux decline. It was shown that all ion exchange pretreatments yielded similar rates of flux decline, however anion exchange pretreated samples yielded overall lower flux. Therefore, removal of divalent cations could result in a decrease in fouling of RO compared to the removal of DOM.

CHAPTER 1
INTRODUCTION

Climate modeling has concluded that future climate conditions will yield greater demands on water resources than current demands, not including the demands of a larger population and a larger economy [1]. Increases in potable water demand coupled with decreases in source water quality will produce a growing market for future membrane technologies such as nanofiltration (NF) and reverse osmosis (RO).

Other concerns of interest include “emerging contaminants”. Although the toxicity of these constituents is still unknown, it is inevitable that these compounds will be regulated in the future. To prepare for these regulations, it is important to understand which water treatment processes are capable of removing these micropollutants and how that impacts water chemistry. Although both NF and RO have been shown to remove many of these constituents, this research focuses on RO. While RO has been shown to remove many of the micropollutants found in test sites throughout the United States, fouling of RO membranes can be problematic. For fouling of NF with a wastewater, initial stages of fouling are often due to species precipitated with sulfate and carbonate, and at the later fouling stage, complex organics with carboxyl acid, amide, and alkyl halide functional groups deposit on the membrane and form a densely packed fouling layer [2]. This research seeks to address these fouling concerns by removing both the inorganic and the organic fouling constituents with ion exchange pretreatment, and provide new insights into reverse osmosis.

The first portion of this research seeks to address the fundamental question of the changes in water chemistry during ion exchange reactions through the evaluation of the stoichiometric relationships that occur during cation exchange reactions. The

second portion of this research will explore the possibility of utilizing simultaneous cation and anion exchange in the same vessel. The third portion of this research seeks to apply the fundamental knowledge learned in the first two parts to bench-scale membrane experiments. Cation exchange, anion exchange, and combined ion exchange are implemented as pre-treatment options to reverse osmosis in order to evaluate the impact on permeate flux decline.

Therefore, the overarching goal of this research is to understand fundamental chemistry during combined anion and cation exchange reactions in order to reduce membrane fouling by pre-treatment.

CHAPTER 2
ALKALINE EARTH METAL CATION EXCHANGE: EFFECT OF MOBILE COUNTERION AND DISSOLVED ORGANIC MATTER

Background

Increasing population, urbanization, and climate change represent global game changers concerning the future quantity and quality of drinking water supplies [3, 4]. Moreover, anthropogenic activities and climate change are expected to increase the concentrations of dissolved organic matter (DOM) and total dissolved solids (TDS) in existing freshwater supplies [5, 6]. As such, many countries will have to augment their existing drinking water supplies with alternative water sources that are characterized by elevated concentrations of DOM or TDS or both. The use of alternative water sources, such as organic-rich surface water or brackish groundwater, is expected to necessitate advanced water treatment trains in which membrane processes will be an integral part of DOM and TDS removal.

Membrane fouling, product water recovery, and management of membrane concentrate are considered major challenges to efficient and effective membrane separation [7-9]. Water sources that contain both DOM and divalent metal cations (i.e., a subfraction of TDS) are known to be problematic in terms of membrane fouling. For instance, Ca^{2+} can promote the aggregation of DOM molecules and act as a bridge between DOM molecules and the membrane surface, both of which contribute to a dense fouling layer [10-14]. Precipitation of $CaCO_3$, $CaSO_4$, $BaSO_4$, and other sparingly soluble minerals can foul membranes and decrease membrane performance [15, 16]. As a result, various pretreatment processes that target either organic or inorganic foulants have been studied with the goal of reducing membrane fouling [17-19]. There is no consensus, however, on the efficacy of pretreatment processes to reduce membrane

fouling. One reason for the inconclusive results is that pretreatment processes focus on either DOM removal or divalent metal cation removal. For example, both anion exchange and cation exchange have been tested as separate processes for DOM removal and divalent metal cation removal, respectively [20-24]. However, there is limited research investigating combined anion and cation exchange for simultaneous removal of DOM and divalent metal cations during drinking water treatment [25]. The proposed combined ion exchange process uses anion exchange resin and cation exchange resin in a single completely mixed flow reactor or fluidized bed reactor [26]. A majority of the resin is continuously recycled within the reactor while a small fraction of resin is regenerated and returned to the reactor. Anion exchange resin and cation exchange resin exhausted with contaminants are regenerated in a single reactor using a concentrated salt solution. The underlying removal mechanism is stoichiometric exchange between aqueous DOM and chloride on the anion exchange resin and metal cations in solution and sodium on the cation exchange resin. Apell and Boyer tested this novel combined anion and cation exchange process at the laboratory scale and showed 70% dissolved organic carbon (DOC) removal and >55% total hardness removal [25]. The combined ion exchange process is expected to substantially reduce membrane fouling because both organic and inorganic precursors of membrane fouling are removed.

Although the combined ion exchange process was shown to be effective for simultaneous removal of DOC and total hardness from a real groundwater [25], the interactions between divalent metal cations, inorganic anions, DOM, and anion and cation exchange resins were not systematically evaluated. In particular, the real

groundwater was dominated by Ca^{2+} and it is not known how competition with Mg^{2+} or trace concentrations of Sr^{2+} or Ba^{2+} would affect the cation exchange process. Interactions between Ca^{2+} and DOM, and to a lesser extent Mg^{2+} and DOM, have been studied [27-29]. There are fewer studies that have investigated Sr^{2+}–DOM and Ba^{2+}–DOM interactions [30]. There are also few previous studies that have investigated the effects of physical–chemical processes on the alkaline earth metal series [31]. Finally, although there have been advances in DOM removal by anion exchange [32-35], it is not well-documented in the literature how the uptake of divalent metal cations during cation exchange would perform in the presence of DOM. Thus, the gaps in knowledge surrounding combined ion exchange as a new drinking water treatment process motivated this research to evaluate the fundamental interactions that take place during cation exchange. The goal of this research was to provide an improved understanding of the interactions between alkaline earth metals and DOM under conditions that are encountered during drinking water treatment with particular focus on cation exchange. The specific objectives of this research were to (i) quantify the stoichiometry and selective removal of alkaline earth metals during cation exchange; (ii) evaluate the potential for coremoval of DOM during cation exchange; (iii) evaluate the role of precipitation and complex formation reactions during cation exchange; and (iv) discuss the implications of the results for drinking water treatment.

Methods and Materials

Model Waters

Table 2-1 shows the measured composition of all model waters used in this research. The rationale for the composition of the model waters was to approximate a

real groundwater that was previously studied using combined anion and cation exchange [25], and in addition, to vary the speciation of Ca and Mg to represent different sources of hardness in drinking water. The total concentration of divalent metal cations was constant at ~2.5 mmol/L (~250 mg/L as $CaCO_3$), while the speciation of divalent metal cations was varied as follows: Ca only, Ca and Mg, Mg only, and zero divalent metal cations (i.e., Na only). The model waters were prepared by dissolving salts and DOM in deionized (DI) water with no additional pH adjustment. The salts included ACS reagent grade purity $CaCl_2 \cdot 2H_2O$, $MgCl_2 \cdot 6H_2O$, $NaHCO_3$, and Na_2SO_4. The DOM isolates were Suwannee River DOM (SRDOM), International Humic Substances Society 1R101N, and Saint Marys River DOM (StMRDOM) isolated from the Saint Marys River in Florida [36]. The charge density of the DOM isolates was obtained by potentiometric titration described in Appendix A and shown in Figure A-1. Visual MINTEQ was used to evaluate the stability of the model waters as discussed in Appendix A and shown in Tables A-1, A-2, and A-3. The model waters were limited to inorganic cations (Na^+, Mg^{2+}, Ca^{2+}, Sr^{2+}, Ba^{2+}), inorganic anions (Cl^-, SO_4^{2-}, HCO_3^-/ CO_3^{2-}), and DOM because the focus of the work was cation exchange. Although the results of this work have implications for membrane fouling, the model waters did not include all possible foulants such as silica.

Cation Exchange Resin Preparation

Two cation exchange resins were used in this work: MIEX WA172 (hereafter MIEX) and Purolite C106Na (hereafter non- MIEX). Both resins had the same pore structure, polymer composition, and weak-acid functional groups as shown in Table A-4. MIEX resin contained magnetic iron oxide giving it magnetic properties that were not

present in non- MIEX resin. The resins were converted to the following mobile counterion forms: sodium (R-Na), magnesium (R_2-Mg), calcium (R_2-Ca), strontium (R_2-Sr), and barium (R_2-Ba) where R represents either MIEX or non-MIEX resin and the subscript 2 shows that divalent cations occupy two exchange sites on the resin. MIEX and non-MIEX resin were converted to the appropriate mobile counterion by regenerating the resins in a concentrated metal chloride salt solution that contained 25× stoichiometric excess of the target mobile counterion, which was calculated based on the ion exchange capacity of the resins as reported by the manufacturers. The regeneration procedure has been used previously to convert ion-exchange resin to different mobile counterion forms and regenerate exhausted ion-exchange resin [25, 37, 38].

Cation Exchange Experiments

Batch equilibrium experiments were conducted by adding 1.6 mL of MIEX resin or 0.31 mL of non-MIEX resin to 100 mL of model water. The MIEX resin dose was based on DOC removal in previous work [25]. The non-MIEX resin dose was calculated so that both MIEX resin and non-MIEX resin were tested at the same meq/L dose based on the ion exchange capacity of the resins. Accurate and precise dosing of ion-exchange resin on a volumetric basis is challenging for small volumes of resin. As a result, MIEX resin and non-MIEX resin were filtered, dried in a desiccator, weighed on an analytical balance, and added as dry resin based on previous work [32, 33]. Samples were mixed for 2 d on a shaker table at 200 rpm to ensure full equilibrium. The equilibrium time was determined from preliminary kinetic experiments. In practice, ion exchange is a rapid process in which effective treatment is achieved in 60 min or less [26, 39]. All combinations of cation exchange resin and model water were tested in

duplicate. All results show the mean of duplicate samples with error bars showing the standard error as described in Appendix A. All samples were filtered through 0.45-μm nylon membrane filters after 2 d of mixing. The filters were prepared by sequentially rinsing with 500 mL of DI water and ~10 mL of sample. DOC and dissolved inorganic carbon (DIC) were measured by high-temperature combustion on a total organic carbon analyzer (Shimadzu, TOC-VCPH). Ultraviolet absorbance was measured on a UV–visible spectrophotometer (Hitachi, U-2900) at 254 nm (UVA_{254}) using a 1-cm quartz cuvette. Inorganic cations (Na^+, Mg^{2+}, Ca^{2+}, Sr^{2+}, Ba^{2+}) and anions (Cl^-, SO_4^{2-}) were measured by ion chromatography with conductivity detection (Dionex, ICS- 3000). Calibration standards were prepared from appropriate ACS reagent grade purity salts. Operating conditions for ion chromatography are described in Appendix A. An Acumet AP71 pH meter with a pH/ATC probe was used to measure pH.

Results and Discussion

Stoichiometry of Cation Exchange

Ion exchange differs from ordinary adsorption processes in that there is a charge balance during the exchange process in which the total equivalent concentration of ions removed from solution is equal to the total equivalent concentration of ions released from the resin. The cation exchange stoichiometry of MIEX resin for different mobile counterions and under different water chemistry conditions is shown in Figure 2-1. Cation removal and cation release are expressed in meq/L to account for exchange of monovalent and divalent cations. The y = x line represents the stoichiometric exchange of cations in solution with cations on the resin. Data that fall along the y = x line indicate ideal cation exchange behavior.

The results in Figure 2-1 illustrate the following key points. Aqueous Ca^{2+} and aqueous Mg^{2+}, in both the absence and presence of SRDOM, exchanged stoichiometrically with resin-phase Na, Mg, and Sr. The negligible effect of SRDOM on cation exchange stoichiometry was because the meq/L concentration of divalent metal cations was approximately 50× higher than the meq/L concentration of SRDOM (see Table 2-1). All data for MIEX-Ba resin were systematically shifted to the left of the y = x line indicating more cations removed from solution than released by the resin. This typically suggests adsorption, but is most likely indicative of Ba mineral precipitation as discussed in a later section. As expected, there was minimal exchange between aqueous Na^{+} and the resin-phase alkaline earth metals because of the higher selectivity of MIEX resin for divalent cations; as a control there was no change in the solution composition when the aqueous solute and resin-phase counterion were the same species. Additional cation exchange stoichiometry data for MIEX resin in the presence of StMRDOM and non-MIEX resin in the presence of SRDOM are shown in Figures A-2 and A-3. The results follow trends similar to those in Figure 2-1. For instance, ideal cation exchange behavior for R-Na, R_2-Mg, R_2-Ca, and R_2-Sr, and more cations removed from solution than released by non-MIEX-Ba resin suggesting Ba mineral precipitation.

Selective Removal during Cation Exchange

The selective removal of Ca^{2+}, Mg^{2+}, and other metals during cation exchange is well-established using Na as the mobile counterion [40]. However cation exchange treatment is a dynamic process in which the dominant exchange reaction can be between two or more solutes after replacing the mobile counterion. For example, consider cation exchange treatment of groundwater for hardness removal. Mg^{2+}, Ca^{2+},

and possibly Sr^{2+} and Ba^{2+} will first displace resin-phase Na because the resin has higher selectivity for divalent cations than monovalent cations. Then aqueous divalent cations will exchange with resin-phase divalent cations because of differences in concentration and selectivity until equilibrium is established. Hence, there is a need to understand the selectivity of cation exchange reactions for which Na is not the mobile counterion.

Figure 2-2 compares the selective removal of Ca^{2+} and Mg^{2+} during cation exchange for different resin properties and water chemistry. Figure 2-2A through 2-2C correspond to model waters that contain either Ca^{2+} or Mg^{2+} (total concentration ~2.5 mmol/L), whereas Figure 2-2D through 2-2F correspond to model waters that contain equal equivalent concentrations of Ca^{2+} and Mg^{2+} (total concentration ~2.5 mmol/L). The distinction is important because it allows the selective removal of Ca^{2+} and Mg^{2+} to be quantified without and with direct competition. The results in Figure 2-2 are mostly discussed in terms of affinity (i.e., selective removal) because there was sufficient ion exchange capacity to remove all divalent cations from solution (i.e., cation exchange resin = 8.3 meq/L, divalent metal cations ≈5 meq/L).

MIEX resin showed a similar affinity for Ca^{2+} and Mg^{2+} when there was no competition between Ca^{2+} and Mg^{2+} for ion exchange sites and there was no DOM in solution (Figure 2-2A). Competition between Ca^{2+} and Mg^{2+}, and to a lesser extent the presence of SRDOM, resulted in MIEX resin having a greater affinity for Ca^{2+} over Mg^{2+} (Figure 2-2B, 2-2D, 2-2E). The exception was MIEX-Na resin which showed greater affinity for Mg^{2+} over Ca^{2+}. The different affinity of MIEX-Na resin relative to Mg-, Ca-, Sr-, and Ba-forms of MIEX resin illustrates the need to understand ion exchange

behavior for all relevant mobile counterions. Figure A-4 shows the selective removal of Ca^{2+} and Mg^{2+} by MIEX resin in the presence of StMRDOM; the results follow similar trends as MIEX resin in the presence of SRDOM with MIEX-Na resin having a different affinity than the Mg- and Ca-forms of MIEX resin.

Mg-, Ca-, Sr-, and Ba-forms of non-MIEX resin showed a greater affinity for Ca^{2+} over Mg^{2+} in the presence of SRDOM without and with competition between Ca^{2+} and Mg^{2+}. The Na-form of non-MIEX resin showed nearly complete removal of Mg^{2+} and Ca^{2+} so it was not possible to determine an affinity. All mobile counterion forms of non-MIEX resin showed greater removal capacity for Ca^{2+} and Mg^{2+} than the corresponding form of MIEX resin. The higher capacity of non-MIEX resin was most evident when comparing MIEX-Na and non-MIEXNa resins in which non-MIEX-Na resin achieved essentially complete removal of Ca^{2+} and Mg^{2+}, which is reasonable considering the meq/L resin dose was greater than the divalent cation concentration. The doses of the two cation exchange resins were estimated at approximately the same meq/L dose following data from the manufacturers; however, the results suggest that the meq/L dose of non-MIEX resin was greater than that of the MIEX-resin. Non-MIEX resin is commercially available so there is more certainty in its ion exchange capacity whereas the cationic form of MIEX resin is not commercially available. As a result, MIEX resin may have a lower capacity than provided by the manufacturer.

DOM Co-Removal during Cation Exchange

Many types of DOM contain carboxylic acids that are deprotonated at pH8, −COO−, giving DOM a net negative charge [41]. As a result, DOM is effectively and stoichiometrically removed during anion exchange processes (i.e., exchange between

−COO− and resin-phase Cl^-) [33], and there should be no DOM removal during cation exchange processes (i.e., no exchange between −COO− and resin-phase Na^+). However substantial removal of DOC and UVA_{254} was observed during magnetically enhanced cation exchange (i.e., MIEX-Na resin) in previous work [25] and in this study as shown in Figure 2-3.

The baseline condition for the comparison of all results is MIEX resin, Na mobile counterion, zero divalent metal cations, and SRDOM, which resulted in ~20% DOC removal and ~30% UVA_{254} removal (Figure 2-3A). Removal of DOC increased for the following conditions: alkaline earth metal used as mobile counterion < model water contained divalent metal cations. For example, DOC removal was 33−47% (MIEX-Mg, -Ca, -Sr, and -Ba resins and Na model water) < 46−53% (MIEX-Na resin and Ca, Ca/Mg, Mg model waters) < 46−67% (MIEX-Mg, -Ca, -Sr, and -Ba resins and Ca, Ca/Mg, Mg model waters). Although the presence of Ca^{2+} and Mg^{2+} increased DOC removal relative to Na^+, the identity of the divalent metal cation did not significantly affect DOC removal. UVA_{254} followed the same trend as DOC but showed a greater decrease for all conditions for the MIEX resin in the presence of either type of NOM. Aromatic-rich (i.e., UV-absorbing) domains of DOM are known to interact favorably with polymer resins and Ca^{2+} [42, 43], which accounts for the greater reduction in UVA_{254}. Greater removals of DOC and UVA_{254} were measured when Ba was used as the mobile counterion indicative of Ba mineral precipitation.

The potential for co-removal of StMRDOM during cation exchange was evaluated for all model waters but restricted to Na, Mg, and Ca mobile counterions because of a limited amount of DOM isolate. The results for StMRDOM follow the same trends as

SRDOM in terms of the effects of water chemistry and resin properties on DOC and UVA_{254} removal (Figure 2-3B). The key difference in cation exchange behavior between the DOM isolates was greater removal of StMRDOM DOC than SRDOM DOC. Both DOM isolates had similar acidity as illustrated by their potentiometric titrations (Figure A-1). The DOM isolates, however, differed in their specific UVA_{254} ($SUVA_{254}$), which is a widely used surrogate for aromaticity [44]. The $SUVA_{254}$ values for StMRDOM and SRDOM were approximately 6 and 4 L/mg·m, respectively, indicating that StMRDOM was more enriched in aromatic carbon than SRDOM. Thus, the results for StMRDOM follow from the favorable interactions between aromatic domains of StMRDOM with the resin matrix, Ca^{2+}, and other divalent metal cations.

Unlike the results for MIEX resin, there was negligible removal of DOC and UVA_{254} by non-MIEX resin as shown in Figure 2-3C (with the exception of non-MIEX-Ba resin indicative of Ba mineral precipitation). Together, the results for MIEX resin and non-MIEX resin indicate that cation exchange uptake of positively charged metal–DOM complexes or surface complexation between DOM and mobile counterions are not the likely removal mechanisms. Both MIEX resin and non- MIEX resin had similar resin properties (Table A-4). The key difference between the resins was the incorporation of magnetic iron oxide into the polymer matrix of MIEX resin. The magnetic iron oxide allows MIEX resin to have a smaller particle size than traditional ion exchange resins and allows for rapid settling and separation of MIEX resin from solution [45]. There is no previous research examining the role of iron oxide in MIEX resin on DOM removal. Analysis of MIEX resin by vibrating sample magnetometer showed that the iron oxide was synthetic, single domain magnetite with a particle size less than ~200 nm

(Appendix A, Table A-5, and Figure A-5). Magnetite has been used previously to prepare magnetic polymer resins and adsorbents [46, 47]. Previous scanning electron microscope images of anionic MIEX resin showed that the resin surface was highly porous and heterogeneous [37], which suggests that magnetite nanoparticles could be exposed on the resin surface. Thus, the working hypothesis for DOM co-removal during magnetically enhanced cation exchange is adsorption of DOM and metal−DOM complexes to exposed magnetite nanoparticles. The average point of zero charge for synthetic magnetite is 6.8 [48], so at the pH of the model waters, pH 8, the magnetite surface is negatively charged, i.e., Fe−O−. The enhanced adsorption of DOM by MIEX resin in the presence of divalent metal cations in solution suggests that metal−DOM complexes, e.g., Ca^{2+}−DOM, are being removed through electrostatic interactions with negatively charged magnetite. Electrostatic removal of metal−DOM complexes is consistent with previous work showing electrostatic removal of ^{90}Sr by magnetite at alkaline pH [49]. The low DOM removal by MIEX resin in the absence of divalent metal cations is consistent with the limited adsorption of DOM by magnetite at alkaline pH [50]. Understanding the role of iron oxide in MIEX resin is important because magnetically enhanced polymer adsorbents are increasingly being considered for water treatment, separation processes, and drug delivery [51, 52].

Precipitation of Barium Minerals

One of the most striking results from Figure 2-3 was the substantial removal of DOM in experiments in which Ba was used as the mobile counterion and the model water contained divalent metal cations. For example, DOC removal was 61−67% for both MIEX-Ba and non-MIEX-Ba resins in the presence of Ca^{2+} and/or Mg^{2+} (Figure 2-

3A and 2-3C), which was also the maximum DOC removal observed for all test conditions using SRDOM. There was much less DOC removal by MIEX-Ba resin and there was no DOC removal by non-MIEX-Ba resin when divalent metal cations were absent from the model water. Consequently, the working mechanism of DOM co-removal during Ba-form cation exchange is hypothesized to include exchange of aqueous divalent metal cations with resin-phase Ba, release of Ba into bulk solution, precipitation of Ba minerals, DOM coprecipitation with or adsorption to Ba minerals, and DOM removal during solid–liquid separation.

The precipitation of Ba minerals during Ba-form cation exchange is supported by the sulfate data shown in Figure 2-4. The sulfate concentration was decreased by >90% during Ba-form cation exchange in the presence of Ca^{2+} or Mg^{2+}. In the absence of divalent metal cations (i.e., Na^{+} only), there was much less sulfate removal by MIEX-Ba resin and there was no sulfate removal by non-MIEX-Ba resin. There was no change in the sulfate concentration for Na-, Mg-, Ca-, and Sr-form cation exchange for all model waters except MIEX-Sr resin in the presence of Ca^{2+} (Figure A-6), and there was no change in the chloride concentration for all cation exchange experiments (Figure A-7) thus ruling out anion exchange. Finally, Visual MINTEQ was used to model the precipitation potential of the various model waters before and after cation exchange as summarized in Tables A-2 and A-3. Exchange of Ca^{2+} and Mg^{2+} with R_2-Ba resin resulted in release of Ba^{2+} and supersaturated conditions for Barite ($BaSO_4$) and witherite ($BaCO_3$). Hence, all results support the working hypothesis of Ba mineral precipitation during Ba-form cation exchange. Final confirmation of the hypothesis would require collection and analysis of the precipitate, which was not conducted.

Although precipitation of Ba minerals on membrane surfaces is a known problem [9], precipitation of Ba minerals on ion exchange resin, and subsequent fouling of the resin, is not expected to occur because of separation of anions and cations on respective resins. For instance, during the combined ion exchange process sulfate is loaded on the anion exchange resin while barium is loaded on the cation exchange resin. The precipitation of $BaSO_4$ would not occur until the regeneration process in the bulk solution and not on the resin. Ion exchange waste brine and membrane concentrate are high ionic strength solutions favorable for Ba mineral precipitation, whereas natural waters are less favorable for Ba mineral precipitation (Appendix A).

Implications for Drinking Water Treatment

The motivation for this research was a new combined anion and cation process that can simultaneously treat DOM and metal cations [25]. The alkaline earth metals were the target for cation exchange because Ca and Mg are the dominant sources of hardness in drinking water, and Mg, Ca, Sr, and Ba form sparingly soluble carbonate and sulfate minerals that can foul nanofiltration and reverse osmosis membranes thereby affecting contaminant rejection and water recovery. The cation exchange resins were tested using Na, Mg, Ca, Sr, and Ba as mobile counterions to understand the complex reactions that can occur during combined ion exchange treatment. The results of this work are expected to advance two main directions for combined ion exchange: as an alternative to conventional multi-process DOM and hardness removal (e.g., coagulation followed by lime softening) and as a pretreatment process for membranes that removes both inorganic and organic precursors to membrane fouling. Considering combined ion exchange as an alternative to multi-process DOM and hardness removal, the presence of DOM did not adversely affect the removal of Ca^{2+} or Mg^{2+} by cation

exchange. In contrast, precipitative softening is influenced by DOM with softening performance decreasing as DOM concentration increases [43, 53]. Considering combined ion exchange as a pretreatment for membranes, precipitation of sparingly soluble minerals will occur during the regeneration process and not on the resins or membrane surface thus minimizing fouling.

This work can be reasonably extended to combined ion exchange treatment of terrestrially derived DOM from organic matter impacted aquifers and surface waters. The model waters tested had a DOC concentration of 5 mg/L, which is high for groundwater although not unrealistic for aquifers with organic-rich sediment or impacted by surface water [54]. In addition, many surface waters used as drinking water sources have DOC concentrations of ~5 mg/L. SRDOM and StMRDOM are representative of terrestrially derived DOM found in surface water. Microbially derived DOM, such as wastewater effluent organic matter, was not investigated. Key differences between microbially and terrestrially derived DOM include aromatic carbon content and carboxyl acidity with microbially derived DOM lower in both [55, 56]. Aromatic hydrocarbons and carboxylic acids in terrestrially derived DOM lead to favorable interactions with divalent metal cations, mineral surfaces, and ion exchange resins [42, 43]. Thus additional work is needed to understand the applicability of the results to microbially derived DOM, such as membrane pretreatment for wastewater applications.

This work is specific to cation exchange resin with macroporous structure, polyacrylic composition, and carboxylic acid functional groups. Alternative cation exchange resin properties include gel structure, polystyrene composition, and sulfonic acid functional groups [39, 40]. Cation exchange reactions between Na, Mg, Ca, Sr, and

Ba are not expected to be affected by these changes in resin properties. However, DOM uptake by anion exchange resin is affected by pore structure and polymer composition. For instance, gel resins can limit DOM uptake through size exclusion and polystyrene resins show favorable intermolecular attractions with DOM [42, 57]. Thus, this work is expected to be applicable to other cation exchange resin properties with the caveat that gel- or polystyrene-type cation exchange resins could exhibit size exclusion or enhanced interactions or both with metal–DOM complexes.

Table 2-1. Composition of synthetic model waters used in cation exchange experiments.

test water	pH	Na^+	Mg^{2+}	Ca^{2+}	Cl^-	SO_4^{2-}	DIC	DOC	DOC
		mmol/L	mmol/L	mmol/L	mmol/L	mmol/L	mg/L	mg/L	meq/L
Ca–SRDOM	8.26[a]	3.385[a]	–	2.450[a]	4.654[a]	0.436[a]	27.39[a]	5.02[a]	0.050[a]
	8.46[b]	3.293[b]	–	2.601[b]	4.778[b]	0.451[b]	28.44[b]	4.97[b]	0.051[b]
Ca–StMRDOM	8.09[c]	3.793[c]	–	2.758[c]	4.601[c]	0.441[c]	27.76[c]	4.99[c]	0.055[c]
	8.19[d]	3.419[d]	–	2.485[d]	4.812[d]	0.438[d]	27.15[d]	5.11[d]	0.056[d]
Ca–no DOM	nm	3.380[e]	–	2.026[e]	4.754[e]	0.440[e]	18.89[e]	–	–
	8.04[f]	3.445[f]	–	2.120[f]	4.236[f]	0.445[f]	20.30[f]	–	–
Ca/Mg–SRDOM	8.55[a]	3.391[a]	1.229[a]	1.241[a]	4.697[a]	0.439[a]	27.70[a]	5.47[a]	0.056[a]
	8.51[b]	3.368[b]	1.286[b]	1.362[b]	4.971[b]	0.460[b]	28.39[b]	5.14[b]	0.053[b]
Ca/Mg–StMRDOM	8.14[c]	3.792[c]	1.410[c]	1.425[c]	4.675[c]	0.444[c]	27.60[c]	4.92[c]	0.054[c]
	8.13[d]	3.416[d]	1.241[d]	1.257[d]	4.815[d]	0.438[d]	27.01[d]	5.48[d]	0.060[d]
Ca/Mg–no DOM	nm	3.350[e]	1.219[e]	0.997[e]	4.787[e]	0.443[e]	23.44[e]	–	–
	8.39[f]	3.414[f]	1.235[f]	1.244[f]	4.197[f]	0.442[f]	27.88[f]	–	–
Mg–SRDOM	8.31[a]	3.426[a]	2.466[a]	–	4.727[a]	0.439[a]	27.74[a]	5.29[a]	0.053[a]
	8.57[b]	3.325[b]	2.552[b]	–	4.853[b]	0.449[b]	27.97[b]	5.07[b]	0.052[b]
Mg–StMRDOM	8.21[c]	3.797[c]	2.776[c]	–	4.684[c]	0.445[c]	22.70[c]	5.10[c]	0.056[c]
	8.31[d]	3.419[d]	2.458[d]	–	4.834[d]	0.436[d]	27.42[d]	5.64[d]	0.063[d]
Mg–no DOM	nm	3.417[e]	2.446[e]	–	4.810[e]	0.448[e]	28.22[e]	–	–
	8.43[f]	3.439[f]	2.464[f]	–	4.255[f]	0.452[f]	28.58[f]	–	–
Na–SRDOM	8.29[a]	3.425[a]	–	–	–	0.436[a]	28.06[a]	5.51[a]	0.055[a]
	8.71[b]	3.278[b]	–	–	–	0.446[b]	29.38[b]	5.23[b]	0.054[b]
Na–StMRDOM	8.36[c]	3.811[c]	–	–	–	0.443[c]	28.33[c]	5.23[c]	0.058[c]
Na–no DOM	nm	3.389[e]	–	–	–	0.447[e]	28.67[e]	–	–
	8.63[f]	3.497[f]	–	–	–	0.439[f]	28.94[f]	–	–

a MIEX-Na, Ca, Mg, Sr, and Ba resin forms with Ca, Ca/Mg, Mg, and Na water
b PuroliteC106Na-Na, Ca, Mg, Sr, and Ba resin forms with Ca, Ca/Mg, Mg, and Na water
c MIEX-Na with Ca, Ca/Mg, and Mg water and MIEX-Ca and Mg resin forms with Na water
d MIEX-Ca and Mg resin forms with Ca, Ca/Mg, Mg, and Na water
e MIEX-Na with Ca, Ca/Mg, Mg, and Na water
f MIEX-Ca, Mg, Sr, Ba resin forms with Ca, Ca/Mg, Mg, and Na water
nm = not measured

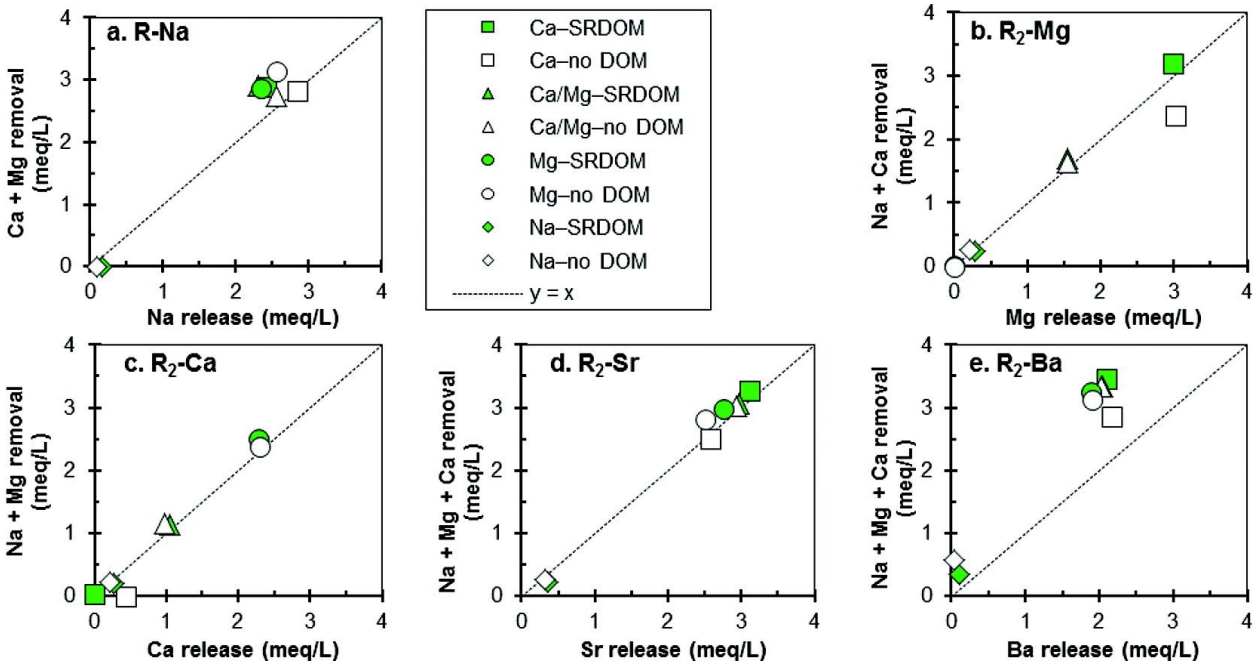

Figure 2-1. Cation exchange stoichiometry for Na-, Mg-, Ca-, Sr-, and Ba-forms of MIEX resin. Legend indicates metal–DOM composition of model water.

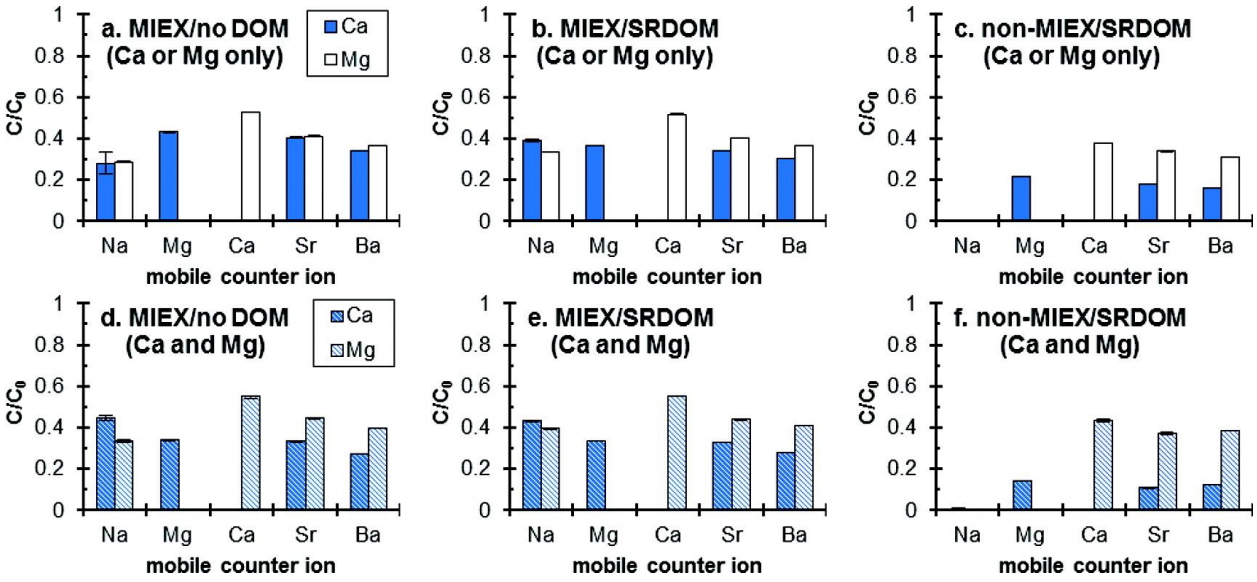

Figure 2-2. Calcium and magnesium removal for Na-, Mg-, Ca-, Sr-, and Ba-forms of resin in the absence/presence of SRDOM. A-C) Ca only or Mg only in aqueous phase (~2.5 mmol/L). D-F) Both Ca (~1.25 mmol/L) and Mg (~1.25 mmol/L) in aqueous phase. Error bars show the standard error for duplicate samples. Magnesium release from Mg-form resin and calcium release from Ca-form resin not shown.

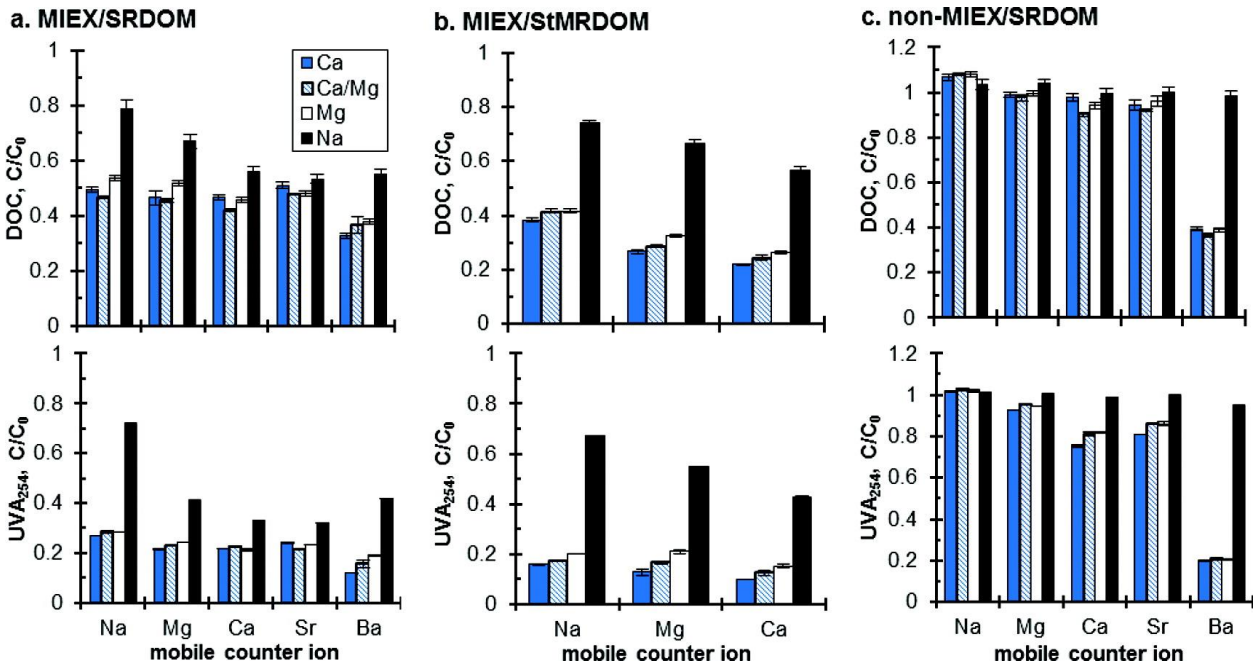

Figure 2-3. Change in DOC and UVA254 during cation exchange uptake of metal cations by Na-, Mg-, Ca-, Sr-, and Ba-forms of resin. A) MIEX resin/SRDOM. B) MIEX resin/StMRDOM. C) non-MIEX resin/SRDOM. Legend indicates cation composition of model water. Error bars show the standard error for duplicate samples.

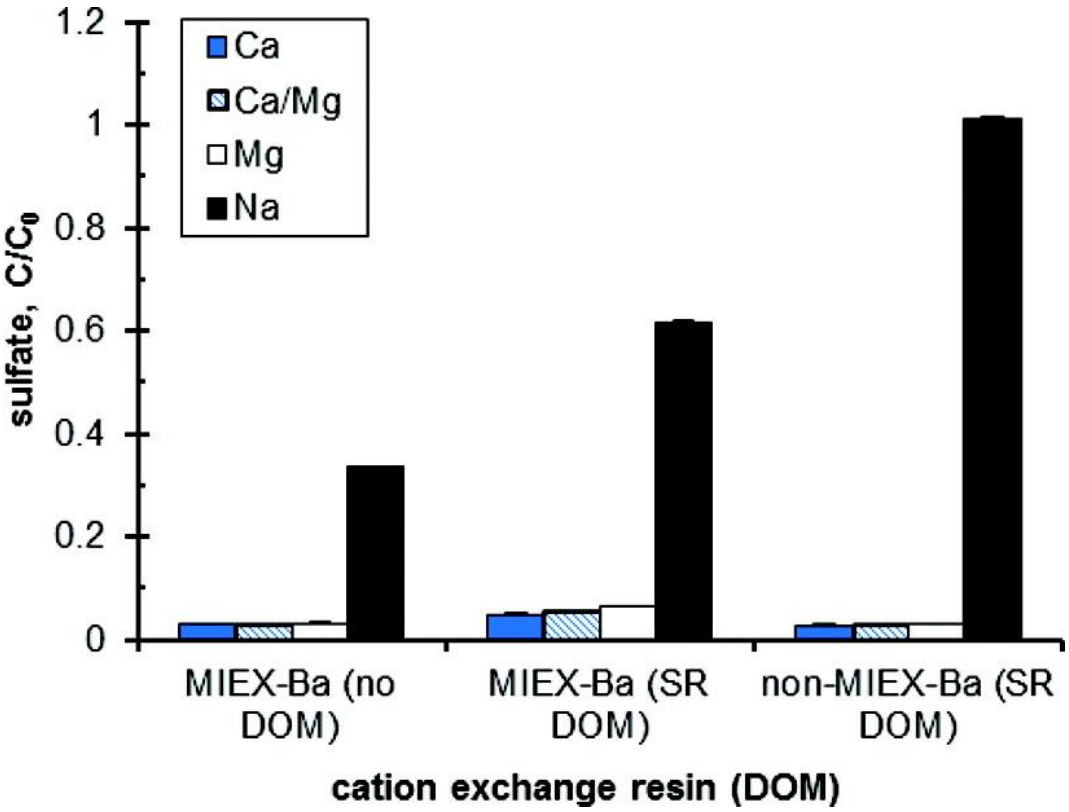

Figure 2-4. Change in dissolved sulfate during cation exchange uptake of metal cations by Ba-form of MIEX and non-MIEX resins in the absence/presence of SRDOM. Legend indicates cation composition of model water. Error bars show the standard error for duplicate samples.

CHAPTER 3
SUPERPOSITION OF ANION AND CATION EXCHANGE FOR REMOVAL OF NATURAL WATER IONS

Background

Inorganic anions and cations as well as dissolved organic matter (DOM) are present in most natural waters. Common inorganic anions present include bicarbonate, sulfate, and chloride, while common cations include calcium, magnesium, and sodium [58]. The source of these inorganic ions includes natural and anthropogenic processes. This research was focused on calcium and magnesium concentrations, which represent the hardness of water. Hard water can cause scaling in hot water tanks, pipes, boilers and washing machines, as well as prevent soaps from lathering. Calcium and magnesium cations can also foul membranes used for removal of pathogenic microorganisms and trace organic chemicals [12, 13, 15]. Therefore, drinking water treatment plants must ensure the proper concentrations of hardness cations because of potential economic, aesthetic, and human health impacts. Groundwater and surface water can have high hardness and hence require the removal of hardness cations (i.e., water softening). Lime softening and cation exchange are the most common processes used in water treatment to remove hardness [39].

DOM is a class of complex organic macromolecules that are ubiquitous in natural waters. Aromatic carbon domains and oxygen, nitrogen, and sulfur functional groups allow DOM to be very reactive although its mass concentration in natural waters is typically much lower than inorganic ions. The anionic nature of DOM is a result of deprotonated carboxylic ($pK_a \approx 3.6–4.8$) [59] and phenolic ($pK_a \approx 8.6–12$) [59] functional groups at the neutral pH of most natural waters. Removing DOM from a natural water source during drinking water treatment is necessary to prevent carcinogenic byproducts

produced after chlorination (i.e., disinfection by-products) [60, 61]. Like divalent cations, DOM can also cause membrane fouling [14, 62-64]. Coagulation is the most common process used to remove DOM. Recent studies, however, have shown anion exchange to be just as effective as coagulation for removal of DOM [65-67].

Ion exchange, which encompasses anion exchange and cation exchange, is a core process to water treatment. The mechanism of ion exchange is weak electrostatically attracted pre-saturant ions on the resin phase exchange stoichiometrically with more desired ions in solution. Ion exchangers can be natural materials (e.g., zeolites, clays, and minerals) or synthetic polymer resins. Ion exchange resins have a polymer structure with attached functional groups that create a fixed charge on the resin. Strong-base anion exchange resin have quaternary ammonium functional groups that give resin fixed positive charge sites and have exchangeable anion (typically chloride) held through electrostatic forces [40]. Chloride on the resin is exchanged with anions such as sulfate and DOM in the aqueous phase. Strong-acid cation exchange resin have sulfonic acid functional groups that give resin fixed negative charge sites and have exchangeable cation (typically sodium) held through electrostatic forces [40]. In solution, the monovalent cation is exchanged for more desirable cations such as calcium and magnesium.

Ion exchange has traditionally been used in drinking water treatment as either anion exchange alone or cation exchange alone. Apell and Boyer explored sequential ion exchange (anion exchange followed by cation exchange and cation exchange followed by anion exchange) as well as combining both anion exchange resin and cation exchange resin in the same vessel (combined ion exchange) [25]. From that

research, hardness cations, DOM, and sulfate were shown to interact differently in separate anion and cation exchange processes when treated sequentially compared to the combined ion exchange process. However, those results were specifically for magnetically enhanced anion (MIEX-Cl) and cation (MIEX-Na) exchange resins. Although MIEX-Cl is more commonly used for drinking water treatment plants, MIEX-Na is not commercially available. This research builds on the feasibility of combined ion exchange with MIEX-Cl and Amberlite 200C-Na, a cation exchange resin commercially available. Much of the focus of the work by Apell and Boyer was on the effects of regeneration on combined *versus* sequential ion exchange [25]. It is not clear from that research as to whether or not combined ion exchange is a linear process; that is, if combined ion exchange would yield the same results as adding the removal of anions from anion exchange and the removal of cations from cation exchange. Mathematically, this is referred to as superposition.

Although ion exchange is a stoichiometric process, not all ions are exchanged equally. Some ions are preferred by the resin over other ions in solution. Divalent ions are typically preferred over monovalent ions, and ions with the same valence have different preferences by the resin depending on properties such as size and hydration [34]. The preference an ion exchange resin can have for one ion over the other is calculated by either a selectivity coefficient or a separation factor [39]. Selectivity coefficients are based on molar concentrations and stoichiometry, and are similar in form to equilibrium constants. Separation factors are calculated based on the distribution of one ion (solid phase divided by solution phase) over the distribution of the other ion. The concentration of DOM is often reported on a mass basis (mg C/L) or

charge basis (meq/L) as opposed to a molar concentration; therefore a separation factor must be calculated to determine an ion exchange resin preference for DOM over another anion. It is not known how the selectivity coefficient and separation factor change during combined ion exchange compared to separate anion and cation exchange.

Implementing combined ion exchange as a full-scale process for drinking water treatment is expected to have several benefits over current approaches to water treatment. For instance, anion exchange could replace coagulation because both processes remove charged portions of organic matter [61, 65] and cation exchange could replace lime softening because both processes remove divalent cations; combining the two ion exchange resins would reduce the process footprint from two vessels to one. This would reduce capital costs, operation and maintenance costs, as well as chemical costs and storage. Removing multiple contaminants (anions and cations, inorganics and organics) in a single process would also generate only one waste stream. In separate ion exchange, two highly concentrated salt tanks are required for the regeneration of each resin. Combined ion exchange has the potential to reduce the chemical requirement of salt, by regenerating all resin in the same tank. Other benefits to combined ion exchange include pretreatment to high pressure membrane systems. Simultaneously removing both anions (e.g., sulfate and DOM) and cations (e.g., calcium) could potentially reduce both inorganic and organic membrane fouling [25].

The goal of this research was to investigate whether the superposition principle applies to removal of natural water anions and cations by ion exchange. The specific

objectives of this research were to quantify 1) stoichiometry, 2) additive removal, 3) effect of DOM, and 4) selectivity coefficients and separation factors during anion and cation exchange. Laboratory experiments were conducted as separate anion exchange, separate cation exchange, and combined anion and cation exchange. Synthetic waters and natural groundwater were used to study the interactions among Na^{+}, Mg^{2+}, Ca^{2+}, Cl^{-}, HCO_3^{-}, SO_4^{2-}, and DOM during ion exchange.

Methods and Materials

Natural and Synthetic Waters

Natural groundwater was collected from Well 3 at Cedar Key Water and Sewer District in Cedar Key, FL, USA and kept at 4˚C before undergoing ion exchange experiments. All ion exchange experiments were conducted at ambient laboratory temperature (approx. 23 °C). Synthetic waters were prepared according to the approximate composition of natural groundwater collected from Well 4 at Cedar Key Water and Sewer District. All prepared samples with their ion compositions are listed in Table 3-1. The source of divalent cations in Cedar Key water is predominantly calcium. The ratio of calcium to magnesium present in synthetic waters was varied to examine the role of calcium and magnesium during separate and combined ion exchange processes. Suwannee River NOM isolate (P/N 1R101N) purchased from the International Humic Substances Society was used for DOM (referred to as SRDOM hereafter). Concentrations of sulfate, bicarbonate, dissolved organic carbon (DOC), and total calcium and/or magnesium remained constant. Stock solutions using ACS reagent grade purity chemicals were prepared by dissolving $CaCl_2 \cdot 2H_2O$, $MgCl_2.6H_2O$, $NaHCO_3$, and Na_2SO_4 in deionized (DI) water. Synthetic waters were prepared by dissolving SRDOM in DI water and then adding appropriate volumes of stock solutions

with no pH adjustment. The source of divalent cations was varied to create synthetic waters with hardness derived from calcium only, calcium and magnesium (in equal molar concentrations), magnesium only, and no hardness (sodium only). Charge density of SRDOM and Cedar Key DOM (CKDOM) was determined by potentiometric titration as reported elsewhere [68, 69].

Ion Exchange Resins and Resin Preparation

MIEX is a magnetically enhanced anion exchange resin (AER) manufactured by Orica Watercare and was regenerated to provide chloride as the presaturant ion. The regeneration procedure followed previous methods [25, 68]. MIEX is a strong-base, macroporous resin with quaternary ammonium functional groups fixed within a polyacrylic matrix and has an anion exchange capacity of 0.52 meq/mL [32]. Amberlite 200C Na is a cation exchange resin (CER) manufactured by Dow and was regenerated to provide sodium as the presaturant ion. Amberlite 200C is a strong-acid, macroporous resin with sulfonic acid functional groups fixed within a polystyrene matrix and has a cation exchange capacity of 1.7 meq/mL based on manufacturer data. MIEX and Amberlite 200C Na are referred to generically as AER and CER, respectively.

The volume of sample water per bottle was 100–200 mL, resulting in a resin dose too small to accurately measure volumetrically. Therefore, all ion exchange resins were dried in desiccators and dosed by mass using experimentally-derived calculations of the density of each of the resins. The resin density was used to convert wet resin dose to dry resin dose according to previous methods [32, 33, 68]. Dry AER was dosed at 0.4978 g/L, which is equivalent to a wet dose of 2 mL/L, as AER is typically used as a slurry. Likewise, dry CER was dosed at 1.7856 g/L, the equivalent to a wet dose of 4 mL/L. Resin doses remained constant during all experiments. Resins and resin doses

were based on previous work conducted by Comstock and Boyer shown to be reasonable resin doses for high hardness and high DOC waters [70, 71].

Batch equilibrium experiments were conducted on a shaker table set at 200 rpm for 2 d. Contact time was established through preliminary kinetic tests that showed less than 1 d to reach equilibrium.

Analytical Methods

All experiments were conducted in triplicate and samples were filtered through 0.45 µm nylon membrane filters (Millipore) prior to analysis. All filters were pre-rinsed with 500 mL of DI water followed by 10 mL of sample. An Accumet AP71 pH meter with pH/ATC probe was used to measure pH. The pH meter was calibrated before each use with pH 4, 7, and 10 buffer solutions. Chloride, sulfate, sodium, calcium, and magnesium were analyzed with ion chromatography (Dionex, ICS-3000) according to previously described methods [68]. Water hardness was determined by the sum of calcium and magnesium. Dissolved inorganic carbon (DIC) was used to determine bicarbonate concentrations, adjusted for the sample pH. DIC and DOC were analyzed by combustion with a total organic carbon analyzer (Shimadzu, TOC-V_{CPH}) with an ASI-V autosampler. All samples ran in duplicate on each instrument and were below 10% relative difference (RD), which was calculated as the absolute difference between replicates divided by the average of the replicates and expressed as percent. Standard calibration checks for both the ion chromatograph and total organic carbon analyzer were within 10% of the known value. UV absorbance at 254 nm (UV_{254}) was measured on a Hitachi U-2900 spectrophotometer using a 1 cm width quartz cuvette. Specific UV_{254} absorbance ($SUVA_{254}$) was calculated as UV_{254}/DOC with units of L/mg·m.

Results and Discussion

Ion-resin Interactions

During ion exchange a charge balance is maintained between the solution and the resin, e.g., for every divalent ion removed from solution, two monovalent ions are released from the resin. This balance in stoichiometry is shown in Figure 3-1, where stoichiometric ion exchange results in data lying exactly on the $y = x$ line (meq/L released into solution equal to meq/L removed from solution and held electrostatically to the resin). Minor deviations from this line are likely experimental variability whereas large deviations indicate processes other than ion exchange. Each data point was determined by the difference in solution concentration before and after ion exchange. The *x*-axis expresses the release of chloride ions during anion exchange processes (Figure 3-1A and 3-1B) and sodium ions during cation exchange processes (Figure 3-1C and 3-1D). The *y*-axis expresses the sum of the anions removed from solution for anion exchange processes (Figure 3-1A and 3-1B) and the sum of cations removed from solution for cation exchange processes (Figure 3-1C and 3-1D).

Figure 3-1A and 3-1B compare the stoichiometry during anion exchange alone to the stoichiometry of anion exchange during combined ion exchange. In Figure 3-1A, two points clearly deviate from the stoichiometric balance of ion exchange; namely, the data points corresponding to the calcium hardness water and the natural groundwater. The source of hardness in Cedar Key water is predominantly calcium; therefore, the synthetic water with calcium hardness is the synthetic water closest in composition to the natural groundwater. These deviations are above the $y = x$ line, indicating more anions being removed than chloride being released. Explanations for the behavior include adsorption, precipitation in the bulk solution, or complex formation reactions.

Adsorption refers to constituents accumulating at or near the surface of the ion exchange resin that does not result in release of presaturant ions. Examples include DOM complexing with the iron oxide within the AER [68]. However, the concentration of DOM is between 0.05–0.06 meq/L compared with other ions in solution between 0.3–3 meq/L. The natural groundwater deviates from stoichiometric ion exchange behavior by 0.7 meq/L and the calcium water deviates by 0.3 meq/L. Therefore, adsorption is not speculated to be the cause of a deviation this significant.

Precipitation occurs when dissolved species become supersaturated (ion activity product is greater than solubility constant) with respect to the solid and form precipitates, or solid compounds. Precipitation in context of this work would occur if supersaturation of dissolved species after ion exchange form precipitates in the bulk solution, or precipitation of salts occur on the ion exchange resin itself during ion exchange; the latter referring to a combination of precipitation and surface adsorption. An explanation of precipitation at the surface of the ion exchange resin is as follows: as sulfate and bicarbonate are exchanged for chloride ions, localized increases in concentrations of these ions occur at the double diffuse layer of the resin. This localized increase in concentrations of bicarbonate could provide appropriate conditions for $CaCO_3$ precipitation when calcium concentrations are adequate with the ion exchange resin acting as the seed for precipitation to occur. This speculation is discussed further in the following section when analyzing anion and cation exchange removal results. It is interesting to note that this phenomenon did not occur during combined ion exchange. It is possible that in combined ion exchange, cations such as calcium are taken up by the

cation exchange resin that is present leaving less calcium available for precipitation in the bulk solution or on the anion exchange resin.

Figure 3-1C and 3-1D compare the stoichiometry during cation exchange alone to the stoichiometry of cation exchange during combined ion exchange. These results are almost identical and reveal that cation exchange alone could almost exactly predict combined ion exchange behavior. It is important to note the magnitude of cation concentrations compared to anion concentrations. Cations are exchanging at approximately 5 meq/L, whereas anions are exchanging at approximately 0.6–0.8 meq/L (the ratio of inorganic cations to inorganic anions is nearly 10 fold). This is important to note because it indicates that the system investigated here is dominated by inorganic cations. Therefore cations may affect anion exchange behavior but anions will not affect cation exchange behavior.

Figure 3-1B and 3-1D compare the stoichiometry of anion exchange and cation exchange during combined ion exchange reactions. Comparing Figure 3-1A and 3-1C to Figure 3-1B and 3-1D, combined ion exchange yields stoichiometric sorption for both anions and cations rather than separate ion exchange processes, where only cations follow stoichiometric sorption. These results are significant and promising for combined ion exchange. Anion exchange alone revealed non-stoichiometric ion exchange behavior with high calcium waters. It appears that combined ion exchange provides stoichiometric ion exchange behavior with varying water conditions, making it a more robust ion exchange process. Although cation exchange alone could precisely predict the behavior of cations during combined ion exchange, the non-stoichiometric behavior of anion exchange alone renders different additive stoichiometry than combined ion

exchange. Therefore, superposition of stoichiometry would not predict stoichiometry of combined ion exchange under certain water chemistry compositions.

Additive Removal of Ion Exchange

An important research question to answer is whether or not the efficiency of combined ion exchange could be estimated by the addition of anion removal and cation removal resulting from separate processes. This new insight could aid in modeling and predicting combined ion exchange behavior [26, 72, 73]. Figure 3-2 expresses the change in concentration (meq/L) of sulfate, bicarbonate, calcium, and magnesium before and after ion exchange for all five waters. Experimental data for anion exchange, cation exchange, and combined ion exchange are reported here, as well as the last bar reflecting theoretical results by adding the results from anion exchange to the results from cation exchange for each of the five sample waters. Error bars for all experimental data are as one standard deviation. Equations for the standard deviation of the difference between the average control sample and the average experimental sample can be found in supplementary material. Theoretical results do not have error bars due to the nature of the data.

Removal of bicarbonate is variable, but certainly more bicarbonate is removed in high calcium hardness waters than any other waters (Figure 3-2A). Results for anion exchange with the synthetic calcium water reveal that more bicarbonate is removed (~0.5 meq/L) than sulfate (< 0.4 meq/L). This is unusual because ion exchange resin prefers ions with the higher charge. However, Figure 3-2B shows approximately 0.5 meq/L of calcium being removed during anion exchange. A divalent cation should not be removed during anion exchange; thus, it is speculated that bicarbonate is gathering in localized areas of the double diffuse layer of the anion exchange resin and creating a

localized IAP > K_{sp} for precipitation of $CaCO_3$. Precipitation in the bulk solution is not hypothesized to occur in combined ion exchange.

Bicarbonate being removed during cation exchange is not reflected in the cation stoichiometry (Figure 3-1C). This is due to the high concentrations of cations relative to anions and can be seen from Figure 3-2: bicarbonate is being exchanged at between 0–1 meq/L but mostly between 0.2 and 0.5 meq/L, whereas calcium and magnesium are being exchanged between 2–5 meq/L.

Figure 3-2B further indicates $CaCO_3$ precipitation during anion exchange with calcium removal during anion exchange in the two high hardness waters (namely, calcium and Cedar Key groundwater). All other calcium removal is as expected and follows rules of superposition. That is, approximately 5 meq/L of calcium is removed during cation exchange and approximately half of that when half the molar concentration of calcium is present.

Magnesium and sulfate removal behavior is stoichiometric and follows the rules of superposition, as well. In fact, magnesium and sulfate removal data reflects little to no other reactions occurring outside of ion exchange. Approximately 4.5 meq/L of magnesium was removed in the synthetic water with magnesium as the divalent cation and about half of that was removed when half the molar concentration of magnesium is present. The natural groundwater had little to no magnesium or sulfate; therefore little to no magnesium or sulfate was removed.

In general, it seems plausible that the removal of sulfate and magnesium during combined ion exchange could be predicted by simply adding anion removal and cation removal. Calcium follows this trend when the calcium concentration is low, but not at

higher concentrations of calcium. Results for bicarbonate removal are variable, but more consistent when lower concentrations of calcium are present.

Effect of Dissolved Organic Matter

Ion exchange removes DOM measured by DOC and UV_{254}. DOC relates to concentration, whereas UV_{254} is indicative of unsaturated carbon bonds and therefore reveals information about the aromaticity of the DOM. Normalizing the UV_{254} absorbance by DOC yields specific UV absorption at 254 nm ($SUVA_{254}$) values. Typical ranges for $SUVA_{254}$ are 0.6–6 L/mg·m [44], with low $SUVA_{254}$ (< 2 L/mg·m) indicating microbially-derived DOM and high $SUVA_{254}$ (> 4 L/mg·m) indicating aromatic, terrestrially-derived DOM [33]. It has also been shown that higher $SUVA_{254}$ is directly correlated with aromatic carbon content and higher molecular weight [44].

Although the concentration of DOM in the experimental waters was low compared to the inorganic ions, these concentrations are realistic for most natural waters. Although low in concentration, DOM tends to be highly reactive. At the neutral pH of most natural waters, acidic groups on DOM deprotonate and allow for electrostatic interactions. Aromatic ring structures and unsaturated carbon allow for non-electrostatic interactions. Results for the removal of DOC are seen in Figure 3-3. Error bars were calculated as described in Figure 3-2. DOC was not removed during cation exchange and therefore results for combined ion exchange mirror those of anion exchange. This is significant because complexation between DOM and divalent cations could allow for cation exchange to remove DOM. These results indicate a lack of complexation with the divalent metal cations investigated here.

Table 3-2 lists all $SUVA_{254}$ values for each of the experimental waters before and after ion exchange. SRDOM is considered an international reference material and end-

member for terrestrial DOM. CKDOM is considered an intermediate, suggesting a mixture of unsaturated and saturated hydrocarbons. $SUVA_{254}$ values in Table 3-2 reflect these sources of composition. DOC was not removed during cation exchange; therefore $SUVA_{254}$ is nearly the same for control samples and cation exchange treated samples (<5% RD for SRDOM and ~6% RD for CKDOM). Combined ion exchange and anion exchange yield the same removal of DOC; therefore $SUVA_{254}$ is almost the same for combined ion exchange treated samples and anion exchange treated samples (<10% RD). This is significant because the same trends in removal hold for model waters as they do for natural water with two different types of DOM.

Selectivity Coefficients

Selectivity coefficients play an important role in many of the modeling techniques for ion exchange, including the use of ion exchange models to predict sorption [74-78]. Ion exchange can be expressed through the following equation, which illustrates an anion exchange process:

$$\beta\overline{A}^{a-} + \alpha B^{\beta-} \leftrightarrow \beta A^{\alpha-} + \alpha\overline{B}^{\beta-} \qquad \text{Eq. 3-1}$$

where α and β are the charge of the ions *A* and *B*, respectively, and the overbars refer to the solid phase of the exchanger. Ion exchange selectivity can be described by a mass action coefficient, termed the selectivity coefficient [79]. At equilibrium, the selectivity coefficient can be described as the conditional equilibrium constant Eq. 3-2 and the separation factor is defined in Eq. 3-3 [39]:

$$K_{A/B} = \frac{[\overline{B}]^{\alpha}[A]^{\beta}}{[B]^{\alpha}[\overline{A}]^{\beta}} = \frac{q_B^{\alpha} C_A^{\beta}}{C_B^{\alpha} q_A^{\beta}} \qquad \text{Eq. 3-2}$$

$$\alpha_{A/B} = \frac{q_B C_A}{C_B q_A}$$ Eq. 3-3

where brackets indicate units of mol/L in the liquid phase and brackets with an overbar indicate units of mol/g in the solid phase, *α* and *β* are defined in Eq. 3-1, *A* is the presaturant ion initially on the ion exchange resin and *B* is the ion removed during ion exchange treatment, *q* is the resin phase concentration at equilibrium (eq/L), and *C* is aqueous phase concentration at equilibrium (eq/L). When ion exchange occurs with two ions of the same charge, e.g., monovalent to monovalent, or divalent to divalent exchange, the separation factor is equal to the selectivity coefficient.

The most preferred ion for the resin would be the ion in combination with the presaturant ion that has the highest selectivity coefficient or separation factor. Not enough information is known regarding DOM to calculate a selectivity coefficient, therefore separation factors were used to evaluate the changes in affinity for various ions during combined ion exchange compared to separate ion exchange. The charge density titration for DOM was used to determine the concentration of DOM in meq/L for each sample point, given the pH of that sample. Table 3-2 lists the separation factor calculated using Eq. 3-3 for each pair of ions for combined ion exchange and separate ion exchange.

The values of separation factors and selectivity coefficients are typically determined through ion exchange isotherms of resin-phase concentration *versus* aqueous-phase concentration, and are typically determined in solutions with only one ion of interest being exchanged. The values presented in this research are therefore not intended to be used as the overall separation factor for these ion exchange processes, but rather a way to compare the separation effect during combined ion exchange to

separate ion exchange. It is a relative comparison under these specific experimental conditions. Comparisons can only be made within each experimental water because ion exchange preference changes as solution concentration (total dissolved solids (TDS)) and/or ionic strength changes.

It can be seen from Table 3-2 that separation from cation exchange to combined ion exchange yielded very similar results. Thus, confirming that separate cation exchange behavior is mirrored in combined ion exchange. Separation of calcium and magnesium indicated the resin has a higher affinity for calcium than magnesium. This can be seen separately in the high calcium water compared to the high magnesium water, as well as when both divalent cations are present in equal molar concentration. The natural groundwater contained little to no magnesium and yielded the same affinity for calcium as the high calcium water.

The trend for lower separation of sulfate and DOM during combined ion exchange than separate anion exchange held true for all experimental waters. Separation factors for bicarbonate during combined ion exchange are similar to those of separate anion exchange for all waters, with slight decreases in the high calcium water and natural groundwater. Results for sulfate with the natural groundwater are inconclusive because little to no sulfate was measured in that water.

Although the affinity of the resin to prefer one ion over the presaturant ion may change from combined ion exchange to separate anion or cation exchange, trends for the overall selectivity sequence did not change. During both separate cation exchange and combined ion exchange processes, with sodium as the presaturant ion, the Amberlite 200C resin selectivity sequence was: $Na^{+} < Mg^{2+} < Ca^{2+}$. During both

separate anion exchange and combined ion exchange processes, with chloride as the presaturant ion, the MIEX resin selectivity sequence was: HCO_3^- < SO_4^{2-} < DOM for both SRDOM and Cedar Key DOM. These results follow general trends in selectivity expected for anion and cation exchange [39].

Final Remarks

The principle of superposition can be applied to anion removal of sulfate and DOC, as well as cation removal of magnesium for combined ion exchange. The principle of superposition can also apply to cation removal of calcium when the initial calcium concentration is < 2.5 meq/L (~50 mg/L).

Combined ion exchange can reduce precipitation of $CaCO_3$ compared to separate ion exchange because calcium is simultaneously removed, thus less is available for precipitation. Under the experimental conditions of the waters tested in this research, $CaCO_3$ was likely to precipitate during anion exchange alone.

Inorganic cations dominate ion exchange behavior during ion exchange reactions and could aid in the prediction of combined ion exchange behavior. Similar trends in ion behavior were seen when comparing synthetic water to a natural groundwater. These results may be different for waters with a higher DOC content, and/or waters with low divalent cations/low TDS.

Combined ion exchange removed ions to an extent greater than or equal to that of separated ion exchange for all ions (both inorganic and organic) with the exception of the removal of bicarbonate in high calcium waters due to precipitation.

DOM properties did not influence the ion exchange behavior in either separate or combined ion exchange. These results could be different for waters with higher DOC content than what was studied here, and/or waters with lower TDS/divalent cations.

Separation factors did not change for cation exchange with combined ion exchange compared to separate cation exchange, but decreased for anion exchange.

Future work is required to determine whether the batch equilibrium data presented in this research could be scaled to a pilot-scale fluidized bed. Regeneration procedures using one salt tank for both anion and cation exchange resins would also need further exploration. Pilot-scale testing is needed to identify the practical advantages and disadvantages of combined ion exchange *versus* separate anion and cation exchange, such as overall footprint of process and precipitation during regeneration.

Table 3-1. Measured composition of synthetic waters and natural water used in ion exchange experiments.

Waters	pH	Na^+ meq/L	Mg^{2+} meq/L	Ca^{2+} meq/L	Cl^- meq/L	SO_4^{2-} meq/L	HCO_3^- meq/L	DOC mg/L	DOC[c] meq/L
Ca hardness [a]	8.1	6.0	-	5.0	4.9	0.91	4.8	5.5	0.054
Ca/Mg hardness[a]	8.2	6.0	2.5	2.5	4.9	0.92	4.9	5.4	0.054
Mg hardness[a]	8.2	6.0	5.0	-	4.8	0.92	4.8	5.6	0.056
No hardness[a]	8.7	5.8	-	-	-	0.91	4.7	5.5	0.057
Cedar Key[b]	8.1	0.26	0.12	4.0	0.44	0.031	4.5	5.7	0.050

[a]Suwannee River DOM
[b]Cedar Key DOM
[c]Converted from mg/L to meq/L by multiplying by the charge density (meq/mg) at the sample pH as determined by potentiometric titration

Table 3-2. Calculated $SUVA_{254}$, ionic strength (I), and separation factors for anion exchange (AEX), cation exchange (CEX), and combined ion exchange (CIX). Test waters: Cedar Key (CK), Ca hardness (Ca), Mg hardness (Mg), Ca/Mg hardness (Ca/Mg), no hardness (No).

Resin-Water	$SUVA_{254}$	Ionic Strength	Separation Factors: resin-phase ion/aqueous-phase ion				
	(L/mg·m)	(mol/L)	Na^+/Ca^{2+}	Na^+/Mg^{2+}	Cl^-/HCO_3^-	Cl^-/SO_4^{2-}	Cl^-/DOC
CIX-Ca	1.2	0.011	220	–	.44	6.9	32
AEX-Ca	1.1	0.013	–	–	1.5	9.4	47
CEX-Ca	4.3	0.011	200	–	–	–	–
Control-Ca	4.2	0.014	–	–	–	–	–
CIX-Ca/Mg	1.2	0.011	340	54	.53	6.8	32
AEX- Ca/Mg	1.2	0.014	–	–	.47	9.2	49
CEX- Ca/Mg	4.2	0.011	290	53	–	–	–
Control- Ca/Mg	4.4	0.014	–	–	–	–	–
CIX-Mg	1.3	0.011	–	49	.47	6.5	33
AEX-Mg	1.2	0.014	–	-	.33	8.4	40
CEX-Mg	4.2	0.011	–	42	–	–	–
Control-Mg	4.3	0.014	–	–	–	–	–
CIX-No	0.9	0.006	–	–	.08	1.8	6
AEX-No	0.9	0.006	–	–	.05	1.9	7
CEX-No	4.2	0.006	–	–	–	–	–
Control-No	4.2	0.006	–	–	–	–	–
CIX-CK	1.1	0.005	200	–[a]	.22	.9	6
AEX-CK	1.1	0.006	–	–	.57	–[b]	7
CEX-CK	3.0	0.005	250	–[a]	–	–	–
Control-CK	2.8	0.007	–	–	–	–	–

[a] No Mg in solution at equilibrium.
[b] No SO_4^{2-} in solution at equilibrium.

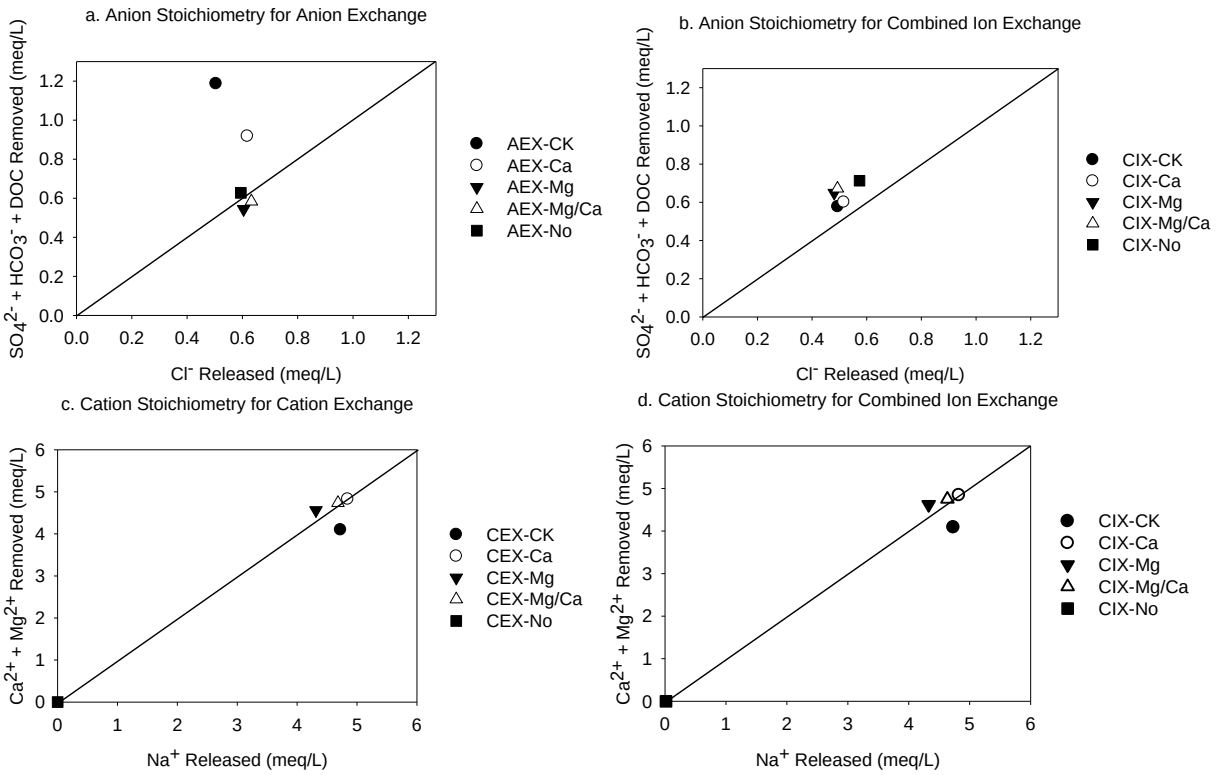

Figure 3-1. Stoichiometry of ion exchange. A) Anion stoichiometry for anion exchange (AEX). B) Anion stoichiometry for combined ion exchange (CIX). C) Cation stoichiometry for cation exchange (CEX). D) Cation stoichiometry for CIX. Test waters: Cedar Key (CK), Ca hardness (Ca), Mg hardness (mg), Ca/Mg hardness (Ca/Mg), no hardness (No).

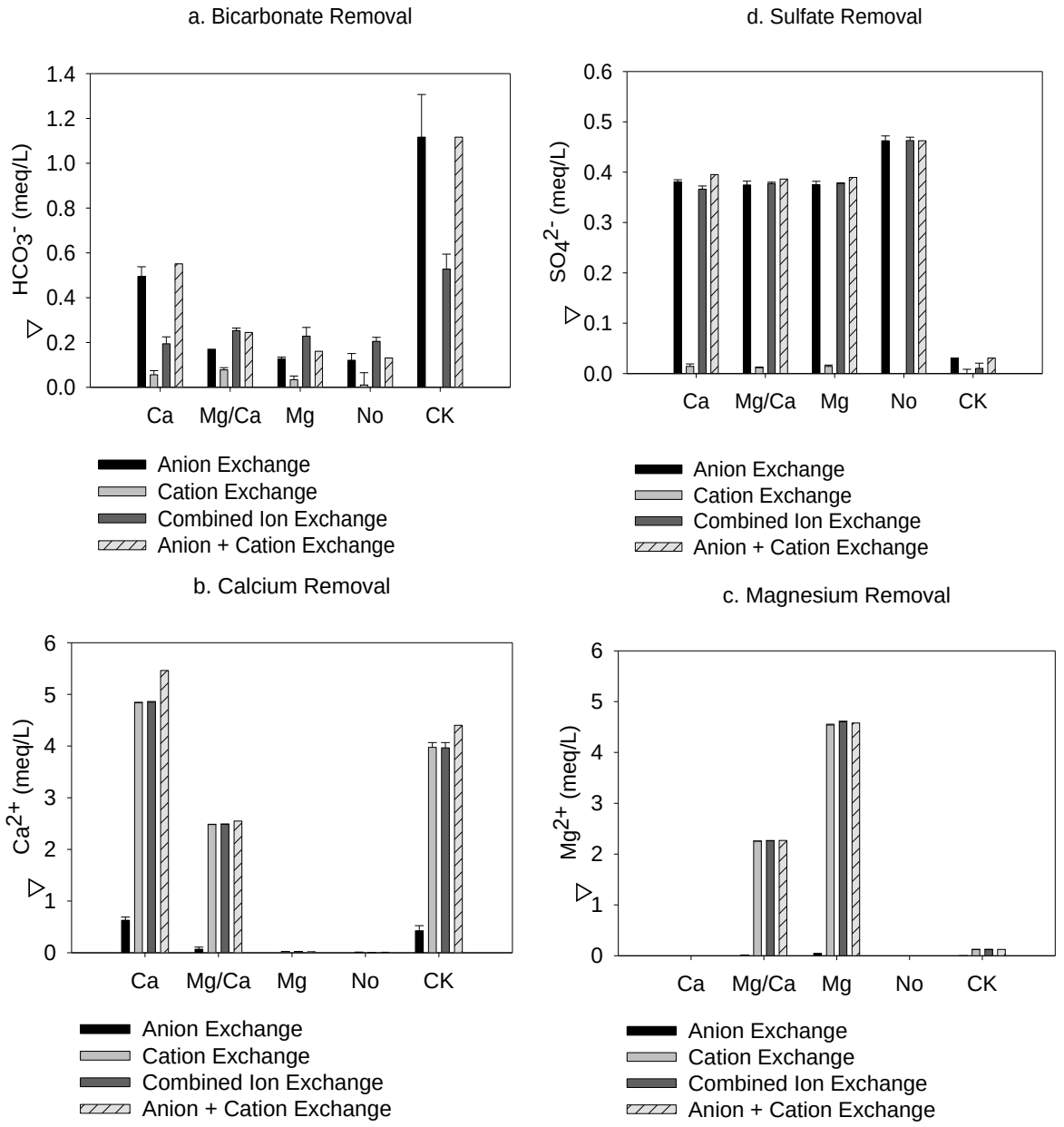

Figure 3-2. Removal of ions in meq/L. A) Bicarbonate removal. B) Calcium removal. C) Magnesium removal. D) Sulfate removal. Test conditions: during anion exchange, cation exchange, combined ion exchange, and theoretical combined ion exchange (i.e., sum of anion exchange and cation exchange). Test waters: Cedar Key (CK), Ca hardness (Ca), Mg hardness (mg), Ca/Mg hardness (Ca/Mg), no hardness (No).

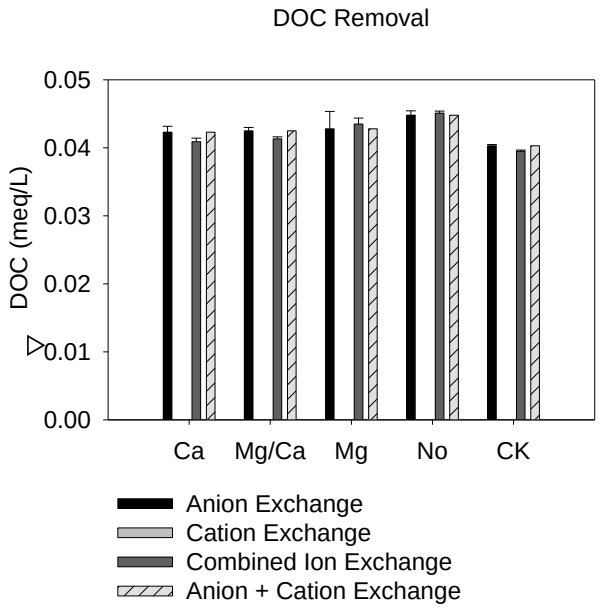

Figure 3-3. DOC removal during anion exchange, cation exchange, combined ion exchange, and theoretical combined ion exchange (i.e., sum of anion exchange and cation exchange). Test waters: Cedar Key (CK), Ca hardness (Ca), Mg hardness (mg), Ca/Mg hardness (Ca/Mg), no hardness (No).

CHAPTER 4
EVALUATION OF ION EXCHANGE PRETREATMENT OPTIONS TO DECREASE FOULING OF A REVERSE OSMOSIS MEMBRANE

Background

Membrane filtration for drinking water treatment has gained considerable attention in the last few decades with a market that is expected to continue to grow. As global warming has led to periods of drought followed by periods of heavy rains, drinking water sources are drastically changing in water quality [3, 4]. In order to meet the demands of these changing water systems, high pressure membrane systems such as reverse osmosis may become a necessary treatment process to a potable drinking water facility. Other factors influencing the need for RO include future regulation of endocrine disrupting compounds, or micropollutants.

Impacts of severe weather events on drinking water sources are not limited to surface water, but can also affect groundwater sources. One such case occurred in Cedar Key, FL, USA, a small town on the coast of north central Florida with groundwater as a source for their drinking water treatment plant. In the summer of 2012, Cedar Key experienced an extended period of drought. This lowered the water table and shifted the salinity line to the well heads for the plant. It became apparent that a reverse osmosis system would need to be implemented in order to reduce the total dissolved solids (TDS) to a level that would meet regulations. In less than six months, this system was installed and delivering safe drinking water to the people of Cedar Key. Soon after, heavy rains aided in shifting the salinity line back toward the shore, and yet Cedar Key Water and Sewer District continued to experience fouling with the RO unit. Although an antiscalant is utilized at the plant, it is clear that inorganic and/or organic fouling is still an issue.

This research focuses on various ion exchange pre-treatment options to reduce fouling of RO systems. Inorganic contaminant removal to reduce inorganic scaling can be accomplished with cation exchange [22]. Natural organic matter (NOM) removal to reduce organic fouling can be accomplished with anion exchange [21]. Combined ion exchange is a novel concept presented by Apell and Boyer [25], and is a feasible option to replace coagulation and lime softening [80].

Ion exchange and RO membranes are complementary processes in that ion exchange releases sodium and chloride when exchanging for less desirable ions in solution such as organic matter and RO removes sodium and chloride without significant fouling of the membrane. Therefore, combined ion exchange has the potential to reduce organic and inorganic fouling of RO, and RO can remove the excess sodium and chloride that is released during combined ion exchange which could potentially harm the distribution system or finished water quality.

Although this relationship seems theoretically sound, the literature suggests that it is not straightforward and is even contradictory in some cases. It is clear from the literature that NOM fouls low and high pressure membranes [14, 81] and divalent cations such as alkaline earth metals can cause scaling on the surface of the membrane when the localized ion activity product exceeds the solubility constant [16, 82]. It is also clear that adding calcium to water with only NOM as the foulant will significantly increase the fouling due to NOM-Ca complexed species [12-14]. However, it is not clear if removing NOM as a pretreatment before RO would, in fact, reduce fouling. NOM can act as an antiscalant by binding to calcium and rendering it less available for precipitation. Likewise, there is very limited research focused on cation

exchange alone as a pretreatment to RO. Subsequently, a direct comparison between anion exchange pretreated samples, cation exchange pretreated samples and combined ion exchange pretreated samples has never been shown in the literature.

Natural water from Cedar Key Water and Sewer District was collected, spiked with NaCl to simulate the salt water intrusion event of 2012, and filtered through a 5 micron filter to simulate cartridge filtration before undergoing RO treatment. Permeate flux decline was measured to compare the performance between anion exchange pretreatment, cation exchange pretreatment, and combined ion exchange pretreatment.

The goal of this research was to directly compare reduction of fouling with these various ion exchange pretreatment schemes on a low-fouling RO membrane. The specific objectives are: 1) to evaluate permeate flux decline; and 2) to investigate changes in water quality due to each ion exchange pretreatment scheme.

Methods and Materials

Experimental Water

Cedar Key Water and Sewer District has an approximately 1 million gallon per day water treatment facility whose source water is a natural groundwater. This groundwater is considered impaired and under the influence of surface water. In general, there is high iron, high alkalinity, elevated hardness, and DOC concentrations averaging 5-6 mg-C/L. Therefore, their water treatment process train includes sodium permanganate injection at the wellhead in order to oxidize the iron, a MIEX process to reduce the high DOC content, lime softening to reduce hardness, gravity filtration, and chlorine disinfection. During the salt water intrusion event of 2012, the TDS reached more than 1300 mg/L with a chloride concentration of approximately 600 mg/L. Samples for this work were collected before and after the MIEX process (raw water with

oxidized iron and anion exchange pretreated water, respectively) and kept at 4˚C before undergoing experiments.

To simulate the salt water intrusion event of 2012, ACS grade NaCl was added to experimental waters to yield a total chloride concentration of 600 mg/L. Chloride concentration of the raw well water was analyzed by ion chromatography with conductivity detection (Dionex, ICS-3000) according to previously published methods [68] and was determined to be 24 mg/L. Therefore, samples were spiked with 576 mg/L chloride. To simulate cartridge filtration before RO, samples were then filtered through a 5 micron polypropylene filter.

Membrane Unit

Membrane experiments were conducted using a Sepa CF II membrane cell system. A 3 horsepower Hydra-cell diaphragm pump was used to pump the sample water to the Sepa cell unit. A refrigerated bath circulator (Neslab RTE20) maintained temperature of 23±1℃ of the sample water in the tank. A Cole-Parmer differential pressure digital flow meter was attached to the permeate line and a surveillance video camera took digital pictures of the permeate flow every five minutes, transmitted in automated e-mails.

A DOW Filmtec XLE4040 reverse osmosis membrane was used throughout this study. This membrane was chosen because it is considered to be an extra low energy, low fouling membrane. It was stored dry and in the dark until RO membrane coupons were cut. These membrane coupons were cut to fit the Sepa CF II membrane cell unit which allows for an effective membrane surface area of 140 cm^2. Coupons were cut from a roll and soaked in deionized water (DI) overnight before each experiment. After presoaking, the RO membrane coupons were placed into the Sepa cell unit, inserted

into the cell holder, and secured by increasing pressure in the cell holder more than 100 psi than the operating pressure by use of a hydraulic hand pump (Enerpac P-142). DI was initially pumped through the membrane for one hour for precompaction. Any change in flow as a result of the compaction of the membrane from operating conditions is adjusted for in this initial step. After precompaction, a preconditioning step was implemented by pumping water with the same ionic strength as the sample water through the membrane for an additional hour. This was made using ACS grade NaCl and DI water to a chloride concentration of 600 mg/L. Therefore, any fouling that would occur with the sample water would not be a result of compaction of the membrane due to pressure or background electrolytes on the surface of the membrane. After precompaction and preconditioning, sample waters were pumped through the membrane overnight. Samples were taken at the initial startup of the sample water, then every hour for six hours after that. Operational pressure was held constant at 200 psi.

Ion Exchange Pretreatment

Samples pretreated by cation exchange were treated by rapid mix with a Phipps and Bird jar tester (PB-700) utilizing freshly regenerated Amberlite 200C-Na resin. Methods for regeneration of Amberlite 200C-Na are reported in Indarawis and Boyer [68]. After spiking with NaCl, samples undergoing cation exchange were exposed to a dose of 4 mL/L resin. Volume is not as accurate as mass, therefore resins were dried according to Indarawis and Boyer [68] and samples undergoing cation exchange were dosed dry at an equivalent wet dose of 4 mL/L. Samples pretreated with anion exchange were treated with 1 mL/L of MIEX resin with chloride as the mobile counterion at the water treatment plant.

Analytical Instruments

Ultra-Violet absorbance at 254 nm (UV_{254}) was measured on a Hitachi U-2900 spectrophotometer using a 1 cm width quartz cell. Electrical conductivity was measured using an ECTestr11 + portable electrode (Eutech Instruments). An Accumet AP71 pH meter with a pH/ATC probe was used to measure pH. The pH meter was calibrated before each use with pH 4, 7, and 10 buffer solutions.

Results and Discussion

Flux Decline

Figure 4-1 shows the flux decline for two raw water samples with no pretreatment, an anion exchange pretreated sample, a cation exchange pretreated sample and a sample subjected to both anion exchange and cation exchange, henceforth referred to as combined ion exchange. The y-axis plots permeate flux (J) normalized to the clean water flux (J_0) recorded during preconditioning. Permeate flux was recorded every five minutes. Small variations in the data could be a result of fluctuations in the temperature of the water or surges from the pump speed. The general trend of the data indicates that, during the first four hours, each water had similar flux behavior; that is, initially increasing before continuously decreasing. After four hours, flux decline showed a linear trend for each of the sample waters. Therefore, regression analysis was conducted from hour 4 until hour 9 in order to quantitatively compare the rate of change in permeate flux for each sample. Figure 4-2 shows the flux decline from hour 4 to hour 9 with regression lines included.

Table 4-2 reports the regression coefficient (b_0), regression slope (b_1), and square of the correlation coefficient (r^2) for the linear regression line constructed for each sample. It is clear from the table that the first sample with no pretreatment did not

fit well to the regression equation (r^2=0.4115). The data associated with this run shows too much scatter and therefore does not fit well with a linear regression model. Therefore, this set of data will be disregarded in the discussion and the second sample with no pretreatment will be considered the baseline (r^2=0.9878). The slope of the regression line following this data set is -0.1259. Therefore, flux decline for Cedar Key groundwater spiked with NaCl and no pretreatment before RO from hour 4 until hour 9 yields a drop in normalized flux of 0.1259 every hour.

Samples pretreated with anion exchange, cation exchange, and combined ion exchange had a very similar rate of decline in flux over time from hour 4 to hour 9 with regression slopes of -0.0794, -0.0729, and -0.0715 respectively. This shows a reduction in flux decline with pretreatment. Although the rate at which flux decline took place for each of the ion exchange pretreatments were the same, there is an initial fouling that occurred with the anion exchange pretreated sample that did not occur with the cation exchange or combined ion exchange pretreated samples. This can be seen in Figure 4-2.

Anion exchange removes significant portions of DOM, therefore remaining ions would predominantly be inorganic cations and fouling would be a result of precipitation from concentration polarization at the surface of the membrane. Cation exchange removes significant portions of inorganic cations, therefore remaining ions of concern would be DOM and fouling would be a result of a possible cake formation on the surface of the membrane. Combined ion exchange removes both DOM and inorganic cations, therefore remaining ions of concern would be very small in concentration. Therefore, a shift in the regression line with the anion exchange pretreated sample indicates

inorganic cations precipitating at the surface of the membrane to be more significant than a possible cake layer formed from DOM. In fact, there is no indication of organic fouling with cation exchange pretreated water since it followed almost exactly the same regression line as the combined ion exchange pretreated sample with DOM removed.

It is important to note that these results may be different for low hardness waters or waters with a lower alkalinity. Cedar Key is a high hardness water with calcium as the source of hardness and high alkalinity. Previous research with this water has shown precipitation of $CaCO_3$ during anion exchange [80]. This precipitation did not occur during combined ion exchange due to the simultaneous removal of anions and cations. It is possible that $CaCO_3$ is the source of fouling with the anion exchange pretreated water, and that this precipitation would not occur with a low hardness water.

Changes in Water Quality

UV absorbance at 254nm

UV_{254} is used as a surrogate measurement of DOM. It is important to note that the cation exchange pretreated sample had a significantly higher initial UV_{254} absorbance than all other samples, including the two raw water samples (Table 4-1). Although most samples were decanted from the top of the collection containers, the sample that underwent cation exchange pretreatment was disrupted in the sample container in transport to the jar tester. This mixed the iron that had settled to the bottom and therefore possibly contained significantly more NOM. However, according to Standard Methods (5910) iron, nitrate, nitrite and bromide are UV-absorbing inorganics that can cause interference with UV-absorption methods. It is possible that the increase in UV absorbance does not reflect an increase in NOM concentration. In either case, it is important to note that with the significant increase in UV_{254}, and potentially the

presence of iron which is a known RO foulant, the cation exchange pretreated sample still performed similar to combined ion exchange and yielded less flux decline than non-pretreated samples.

Conductivity and pH

Conductivity and pH remained fairly constant in the feed water throughout all experiments (Figure 4-3 and Appendix C, respectively). Constant feed water characteristics were important to maintain throughout the experiments to ensure accuracy. Conductivity removal was high for all experiments. These results are expected and indicate the efficient removal of ions accomplished with RO filtration.

Final Remarks

Ion exchange is a viable option for pretreatment to RO membranes. Anion exchange, cation exchange and combined ion exchange showed a decrease in the rate of normalized flux decline than the same water with no pretreatment.

Although the rate of flux decline was the same for all ion exchange pretreatment options, anion exchange pretreated water exhibited an initial fouling shown by a lower overall flux throughout the experiment compared to cation exchange and combined ion exchange pretreated waters.

In high hardness waters, it is possible that inorganic scaling is more severe than organic fouling.

Table 4-1. Initial feed water quality data.

	pH	Conductivity µS/cm	UV_{254} 1/cm
No Pretreatment 1	7.82	2380	0.223
No Pretreatment 2	7.98	2390	0.195
Anion Exchange Pretreated	8.06	2540	0.029
Cation Exchange Pretreated	8.26	2420	0.718
Anion-Cation Exchange Pretreated	8.15	2590	0.055

Table 4-2. Linear regression results for trends in flux decline from hour 4 to hour 9.

	b_0	b_1	r^2
No Pretreatment 1	0.5963	-0.0376	0.4115
No Pretreatment 2	1.214	-0.1259	0.9878
Anion Exchange Pretreated	1.0313	-0.0794	0.9654
Cation Exchange Pretreated	1.1260	-0.0729	0.9213
Anion-Cation Exchange Pretreated	1.1044	-0.0715	0.9450

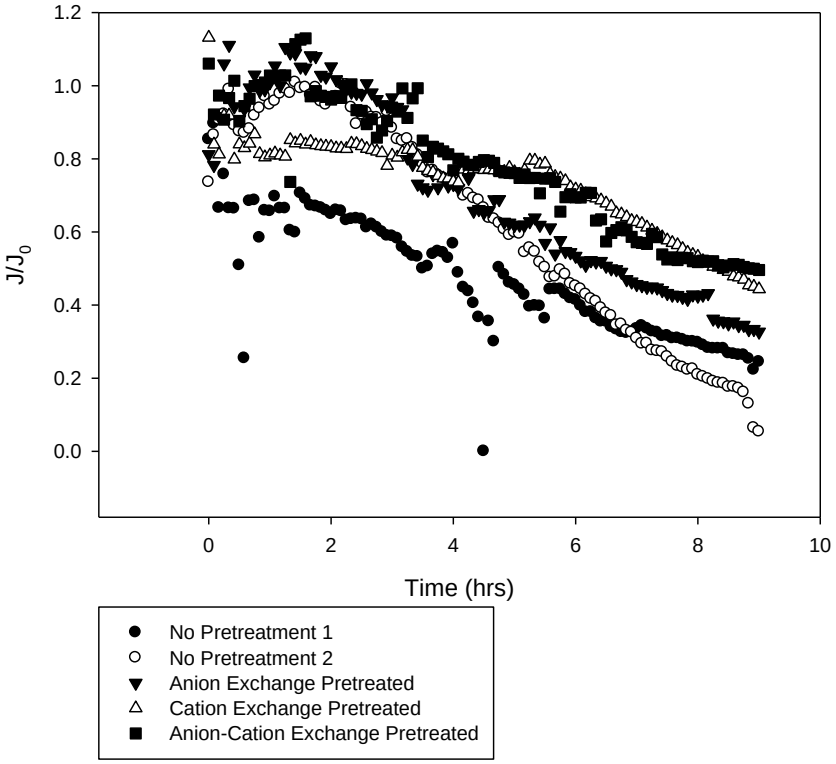

Figure 4-1. Normalized flux decline of ion exchange pretreatments before RO. A) First raw water with no pretreatment. B) Second raw water with no pretreatment. C) Anion exchange pretreatment. D) Cation exchange pretreatment. E) Anion-Cation exchange pretreatment. Test waters: Cedar Key (CK) after sodium permanganate injection (A, B, D) and CK after MIEX (C, E).

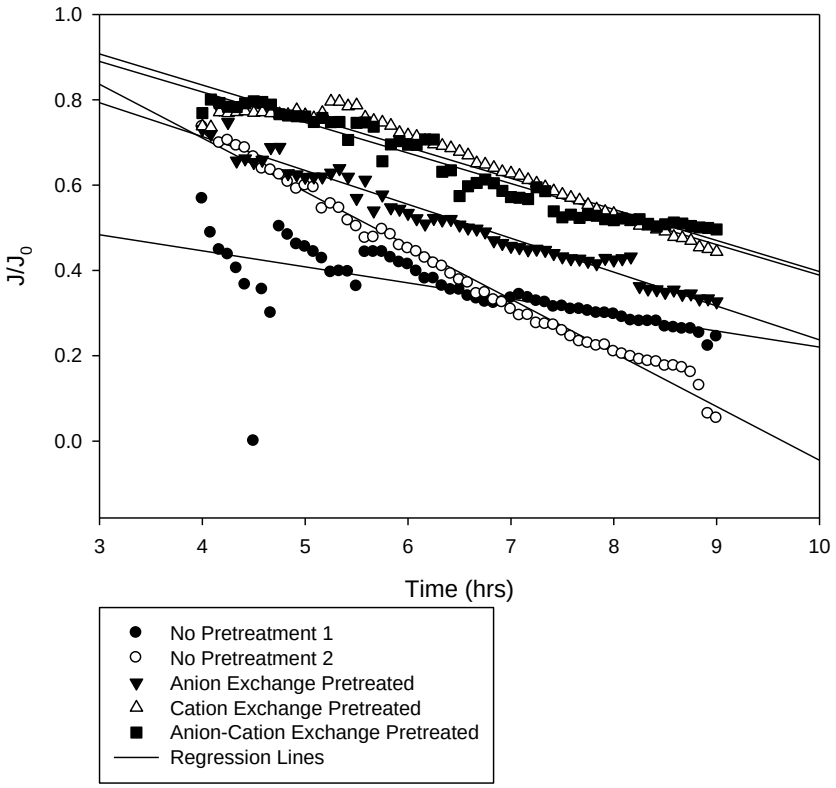

Figure 4-2. Normalized flux decline of ion exchange pretreatments before RO with regression lines from hour 4 to hour 9. A) First raw water with no pretreatment. B) Second raw water with no pretreatment. C) Anion exchange pretreatment D) Cation exchange pretreatment. E) Anion-Cation exchange pretreatment. Test waters: Cedar Key (CK) after sodium permanganate injection (A, B, D) and CK after MIEX (C, E).

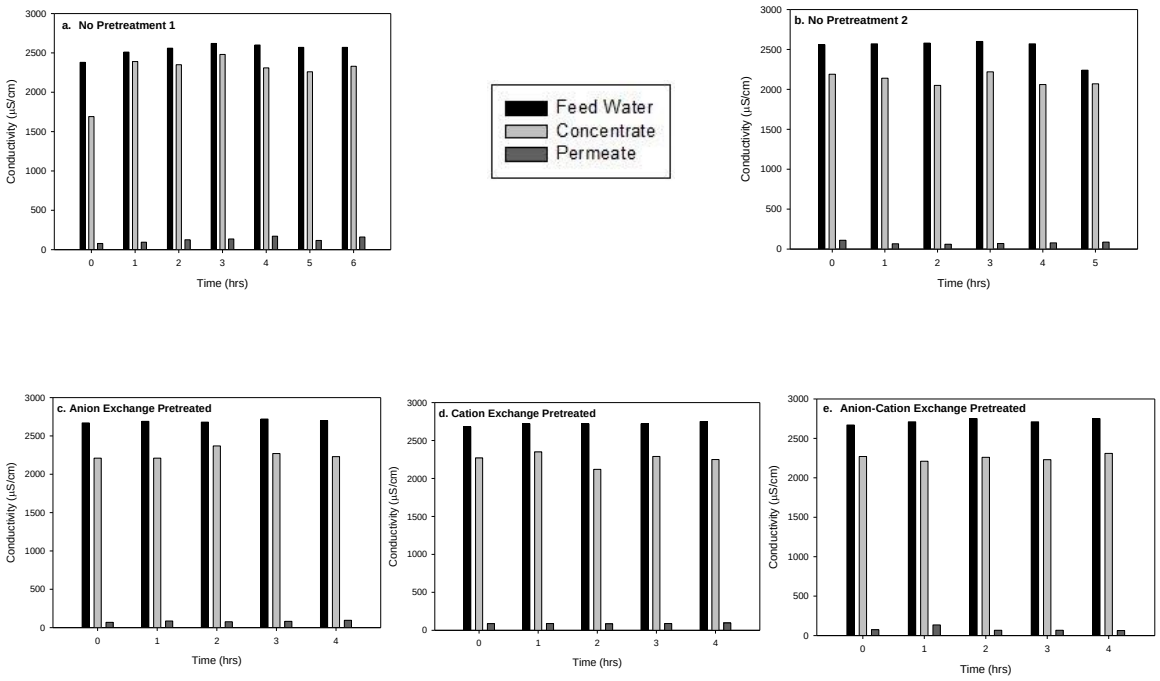

Figure 4-3. Conductivity measurements. A) First raw water with no pretreatment. B) Second raw water with no pretreatment. C) Anion exchange pretreated. D) Cation exchange pretreated. E) Anion-cation exchange pretreated waters. Test waters: feed, concentrate, and permeate.

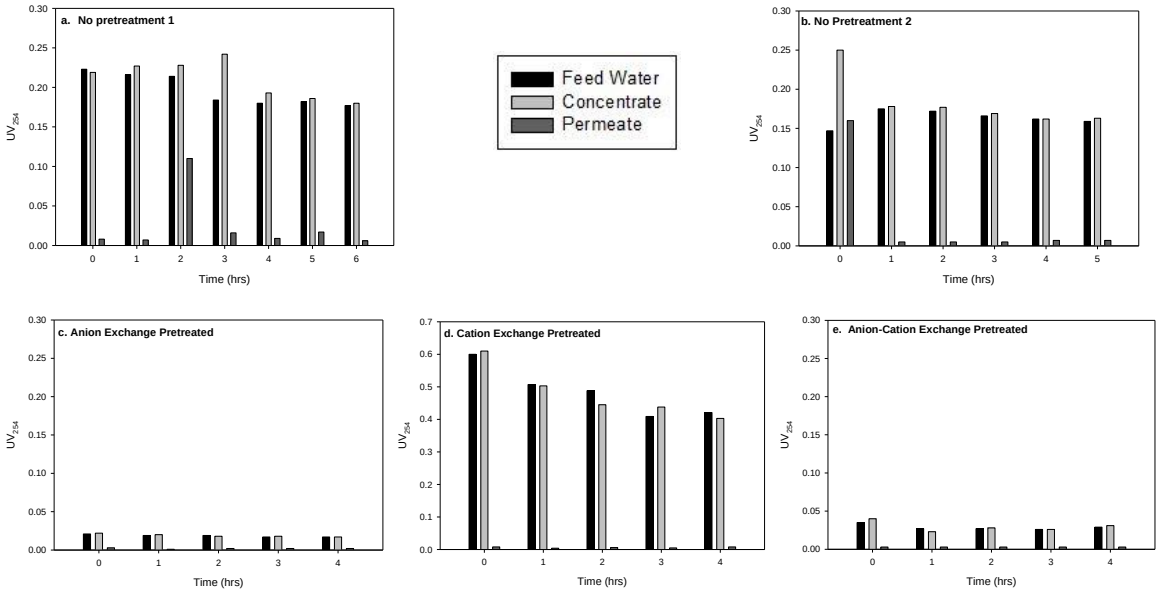

Figure 4-4. UV_{254} measurements. A) First raw water with no pretreatment. B) Second raw water with no pretreatment. C) Anion exchange pretreated. D) Cation exchange pretreated. E) Anion-cation exchange pretreated waters. Test waters: feed, concentrate, and permeate.

CHAPTER 5
CONCLUSIONS

Ion exchange is a viable option for pretreatment to RO membranes. Anion exchange, cation exchange and combined ion exchange showed a decrease in the rate of normalized flux decline than the same water with no pretreatment. Although the rate of flux decline was the same for all ion exchange pretreatment options, anion exchange pretreated water exhibited an initial fouling yielding a lower overall flux throughout the experiment compared to cation exchange and combined ion exchange pretreated waters.

Combined ion exchange reduces precipitation reactions by simultaneously removing anions and cations, thus serving as a robust ion removal treatment process that could replace coagulation and lime softening. Removal of anions by anion exchange and removal of cations by cation exchange can be added to predict the removal accomplished in combined ion exchange for sulfate, magnesium, DOM, and calcium – when the initial calcium concentration is less than 2.5 meq/L (~50 mg/L). Combined ion exchange removed ions to a greater or equal extent than separate ion exchange for all ions (both inorganic and organic) with the exception of bicarbonate in high calcium waters. DOM properties do not influence the ion exchange behavior in either separate or combined ion exchange.

Exposed iron oxide within MIEX ion exchange resin plays a role in DOM removal. NOM binds to $BaSO_4$ either by coprecipitation or adsorption.

APPENDIX A
SUPPLEMENTARY INFORMATION FOR CHAPTER 2

Potentiometric Titration

The potentiometric titration procedure was based on previous work [32]. A 50 mL concentrated dissolved organic matter (DOM) solution was prepared with 15 mg of DOM isolate yielding a concentration of 300 mg/L, 0.1 mol/L KCl, and deionized water. The solution was covered with parafilm and purged with N_2 gas for 30 min to eliminate interference by CO_2, while continuously stirring on a stir plate. After 30 min, the pH was measured and recorded. Subsequent measurements of pH were recorded after 0.04 mol/L NaOH was titrated into the solution in 0.1 mL increments and allowed to equilibrate for 1 min. The charge density was determined by the following equation:

$$\text{DOM charge density (meq/g C)} = \frac{[H^+]+[Na^+]-[OH^-]}{DOC} \quad \text{Eq. A-1}$$

where $[H^+]$, $[Na^+]$, and $[OH^-]$ are in meq/L and DOC is in g-C/L.

Visual MINTEQ

Data collected for the control model waters (i.e., no cation exchange treatment) were analyzed using Visual MINTEQ version 2.6 to compare measured data with theoretical predictions. Due to the complex nature of DOM, this could only be performed for the control model waters with no DOM. For all Visual MINTEQ runs, the system was set to be open to atmospheric CO_2 pressure (0.00038 atm); alkalinity was specified as mg/L as bicarbonate through the parameters menu and not entered as an ionic species in the list of components; activity coefficients were calculated using the Davies equation. All ion concentrations were entered in millimolal units. The stability of the model waters in the absence of cation exchange reactions is shown in Table A-1. For control model waters containing Ca hardness, the DIC predicted by Visual MINTEQ was lower than

the DIC measured. For the control model waters containing Mg hardness or no hardness, the DIC predicted by Visual MINTEQ was in agreement with the DIC measured. Although Visual MINTEQ predicted the precipitation of $CaCO_3$ in Ca containing model waters, the DIC data before and after cation exchange do not indicate carbonate mineral precipitation.

Table A-2 shows the theoretical composition of the model waters used in the chemical equilibrium calculations to understand the precipitation potential following cation exchange. Visual MINTEQ was used to predict the precipitation potential for the model waters in Table A-2. The system was set to be open to atmospheric CO_2 pressure (0.00038 atm); alkalinity was specified as mg/L as bicarbonate through the parameters menu and not entered as an ionic species in the list of components; activity coefficients were calculated using the Davies equation. Each model water in Table A-2 was run under two different settings: (i) no precipitation allowed in order to calculate the saturation index and (ii) precipitation allowed in order to quantify how much solid would theoretically precipitate. Results are shown for model waters that did not contain DOM due to the complicated chemistry of DOM during precipitation reactions. To understand the potential of Ba mineral precipitation after cation exchange experiments, an assumption was made that all divalent cations in the initial model water would be exchanged with Ba or Sr depending on which cation was the mobile counter ion during the reaction. The results of replacing the initial concentration of divalent metal cations with Ba or Sr are reported in Table A-3.

Theoretical results show that $CaCO_3$ (calcite) would precipitate in the model waters with Ca as the only source of divalent metal cations, and that $CaMg(CO_3)_2$

(dolomite) would precipitate in model waters with equal amounts of Ca and Mg as the divalent metal cations. Replacing the divalent metal cations with Ba resulted in theoretical precipitation of $BaSO_4$ (barite) and $BaCO_3$ (witherite). Likewise, replacing the divalent metal cations with equivalent concentrations of Sr resulted in theoretical precipitation of $SrSO_4$ (celestite) and $SrCO_3$ (strontianite). Although mineral precipitation was thermodynamically favorable in most model waters, the Ba-form cation exchange resin in the presence of divalent cations were the only data to consistently support mineral precipitation.

Cation Exchange Resins

Properties of the cation exchange resins are listed in Table A-1. Data for MIEX WA172 (i.e., MIEX resin in article) are from Apell and Boyer [25]. Data for Purolite C106Na (i.e., non-MIEX resin in article) are from the manufacturer.

Standard Error

The error bars in Figures 2-2 through 2-4 show the standard error (SE) calculated as[83]:

$$SE = \frac{s_{C/C_0}}{n} \qquad \text{Eq. A-2}$$

where n = number of duplicates and s_{C/C_0} = standard deviation associated with C/C_0 calculated as follows:

$$s_{C/C_0} = \left(\frac{1}{\sqrt{n}}\right)\left(\frac{C}{C_0}\right)\left(\frac{s_C^2}{C^2} + \frac{s_{C_0}^2}{C_0^2}\right)^{1/2} \qquad \text{Eq. A-3}$$

Ion Chromatography

Operating conditions for cation analysis were as follows: IonPac CG12A guard column and CS-12A analytical column; cation self-regenerating suppressor set to 59 mA; column and detector compartments set to 30°C; eluent composition 20 mM

methanesulfonic acid (prepared by dilution of concentrated methanesulfonic acid); eluent flow rate 1.0 mL/min; and 25 µL sample loop. Operating conditions for anions analysis were as follows: IonPac AG22 guard column and AS-22 analytical column; anion self-regenerating suppressor set to 31 mA; column and detector compartments set to 30°C; eluent composition 4.5 mM Na_2CO_3/1.4 mM $NaHCO_3$ (AS-22 eluent concentrate, Dionex); eluent flow rate 1.2 mL/min; and 25 µL sample loop.

Stoichiometry of Cation Exchange

Results supporting the cation exchange stoichiometry of MIEX resin and non-MIEX resin are shown in Figures A-2 and A-3.

Selective Removal during Cation Exchange

Results supporting removal of Ca^{2+} and Mg^{2+} during cation exchange are shown in Figure A-4.

Magnetic Properties of MIEX Resin

MIEX-Na and MIEX-Ca resins were analyzed on a vibrating sample magnetometer (Princeton Measurements Corporation). The measurement range for this instrument is 5×10^{-5} electromagnetic unit (emu) to 10 emu full scale (SI unit: 10^{-3} $A\cdot m^2$ = 1 emu). The sensitivity is 5×10^{-7} emu standard deviation, 1 second per point. A MIEX-Na resin sample (29.7 mg not including the gel cap) and a MIEX-Ca resin sample (40.4 mg not including the gel cap) were analyzed at magnetic field increments of 1 to 10 mT. Hysteresis loops of both resins samples showed similar magnetic properties as described in Table A-5. Although identifying minerals based on their magnetic properties is an active area of research, the hysteresis properties of MIEX-Na and MIEX-Ca resins (i.e., $M_{rs}/M_s \approx 0.5$ and $H_{cr}/H_c \approx 1.25$) are consistent with single-domain magnetite (Fe_3O_4) with a particle diameter (nonequidimensional, elongated) less than

approximately 0.2 μ m [84-86]. In addition to the data provided by the hysteresis loops, Mayergoyz developed a method using first order reversal curves (FORCs) to further represent hysteresis data [87]. The MIEX resin samples were subjected to a saturating field, as in hysteresis experiments, then lowered to a fraction of the original force, then increased again to saturation. The magnetization curve between the point the field was lowered to and the final point it was brought to for saturation is a FORC. A series of FORCs was generated to construct the contour plot in Figure A-5. This FORC diagram closely matches that of a single-domain magnetic particle prepared by Eastman Kodak Company Research Laboratories [88], and supports the notion that the magnetic particles in MIEX resin are single domain, synthetic magnetite.

Precipitation of Barium Minerals

Results supporting the precipitation of Ba minerals during cation exchange are shown in Figures A-6 and A-7.

Strontium and Barium Precipitation in Natural Waters

Sr and Ba occur in most natural waters. Mean surface water concentrations for Sr and Ba are 1.1 mg/L and 10–60 µg/L, respectively [89, 90]. The ion activity product for $SrSO_4$ (celestite) and $BaSO_4$ (barite) can be calculated using the mean concentration for sulfate in natural waters (20 mg/L) [91]. The ion activity product for celestite is 2.6×10^{-9} ($Ksp = 10^{-6.50}$) [91]. The ion activity product for barite is 1.5×10^{-11} to 9.1×10^{-11} ($Ksp = 10^{-9.96}$) [91]. These calculations illustrate that Sr and Ba will not precipitate under ‘average’ natural water conditions. Ionic strength and temperature were neglected in these calculations and can have an impact on the solubility of these minerals.

Table A-1. Stability of control model waters.

	DIC, mg/L		pH	
	Actual	Visual MINTEQ	Actual	Visual MINTEQ
Ca - no DOM[a]	19	9	nm	8.1
	20	10	8.0	8.1
Ca/Mg - no DOM[a]	23	11	nm	8.1
	28	12	8.4	8.2
Mg - no DOM[a]	28	25	nm	8.5
	29	26	8.4	8.5
Na - no DOM[b]	29	29	nm	8.6
	29	31	8.6	8.6

[a] DIC after cation exchange (MIEX-Na, -Mg, -Ca, -Sr, and -Ba resins/no DOM) was 25–27 mg/L.
[b] DIC after cation exchange (MIEX-Na, -Mg, -Ca, -Sr, and -Ba resins/noDOM) was 23–30 mg/L.
Not measured (nm).

Table A-2. Theoretical composition of initial synthetic model waters with no DOM and varying divalent metal cations.

test waters	**Na^+**	**Ca^{2+}**	**Mg^{2+}**	**Cl^-**	**SO_4^{2-}**	**alkalinity**
	mmol/L	mmol/L	mmol/L	mmol/L	mmol/L	mg/L as HCO_3^-
Ca–no DOM	3.5	2.5	0	5	0.5	153
Ca/Mg–no DOM	3.5	1.25	1.25	5	0.5	153
Mg–no DOM	3.5	0	2.5	5	0.5	153
Na–no DOM	3.5	0	0	0	0.5	153

Table A-3. Results of Visual MINTEQ simulations.

test waters	mineral with the potential to precipitate[a]	saturation index[a,b]	theoretical solid that would form[c]	equilibrium solid amount (mmol/L)[c]
Ca–no DOM	Aragonite	1.004	Calcite	0.884
	Calcite	1.148		
	Vaterite	0.581		
Ca/Mg–no DOM	Aragonite	0.714	Dolomite (ordered)	0.391
	Calcite	0.858		
	Dolomite (disordered)	1.306		
	Dolomite (ordered)	1.856		
	Vaterite	0.292		
Mg–no DOM	Magnesite	0.161		
Na–no DOM	–	–	–	–
Ba in exchange with Ca and Mg	Barite	3.635	Barite	0.520
	Witherite	1.291	Witherite	0.878
Sr in exchange with Ca and Mg	Celestite	0.245	Celestite	0.0734
	Strontianite	1.972	Strontianite	1.09

[a] No precipitation allowed.
[b] $\log(IAP/K_{s0})$; where IAP is the ion activity product and K_{s0} is the stability constant of the solid.
[c] Precipitation allowed.

Table A-4. Properties of cation exchange resins.

resin	pore structure	polymer composition	weak-acid functional groups	capacity (meq/mL)	other
MIEX	macroporous	polyacrylic	carboxylic acid	~0.5	contains magnetic iron oxide
WA172					
Purolite C106Na	macroporous	polyacrylic	carboxylic acid	2.7	non-magnetic polymer

Table A-5. Magnetic properties of MIEX resin.

MIEX resin	**M_{rs}**	**M_s**	**M_{rs}/M_s**	**H_{cr}**	**H_c**	**H_{cr}/H_c**
	$\mu A \cdot m^2$	$\mu A \cdot m^2$	–	mT	mT	–
MIEX-Na	242.9	555.4	0.4373	48.75	36.48	1.336
MIEX-Ca	301.3	664.3	0.4536	47.28	36.73	1.287

Saturation remanence (M_{rs}), saturation magnetization (M_s), remanent coercive force (H_{cr}), ordinary coercive force (H_c).

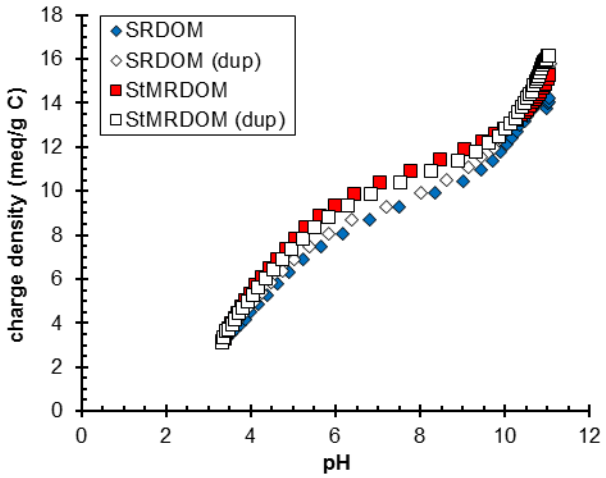

Figure A-1. Charge density of SRDOM and StMRDOM determined from potentiometric titration results. Titrations were conducted in duplicate with good agreement between duplicates as shown.

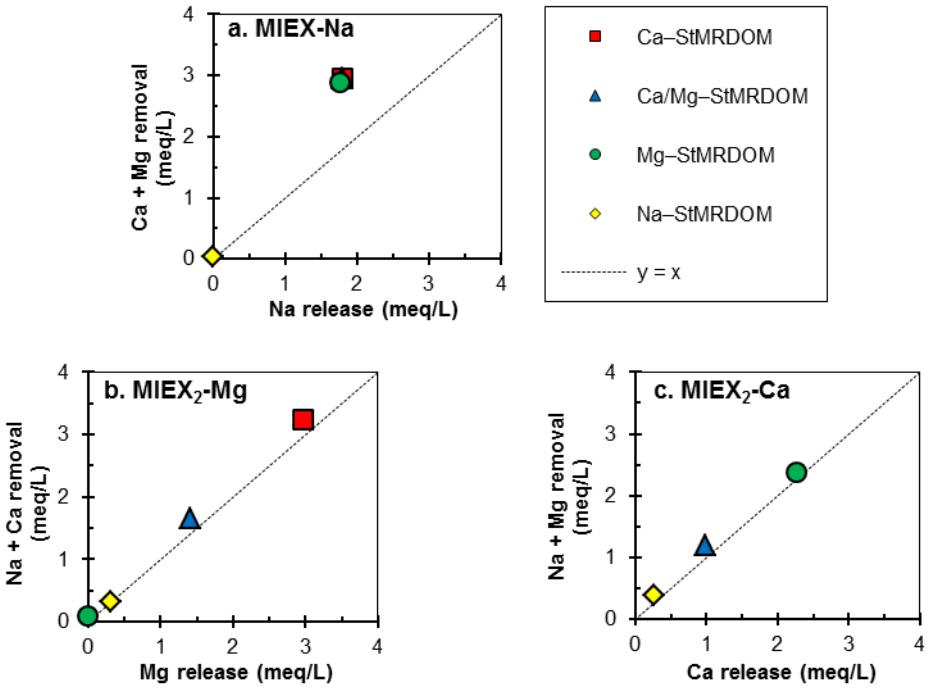

Figure A-2. Cation exchange stoichiometry for Na-, Mg-, and Ca-forms of MIEX resin under varying conditions of metal cations and StMRDOM in solution.

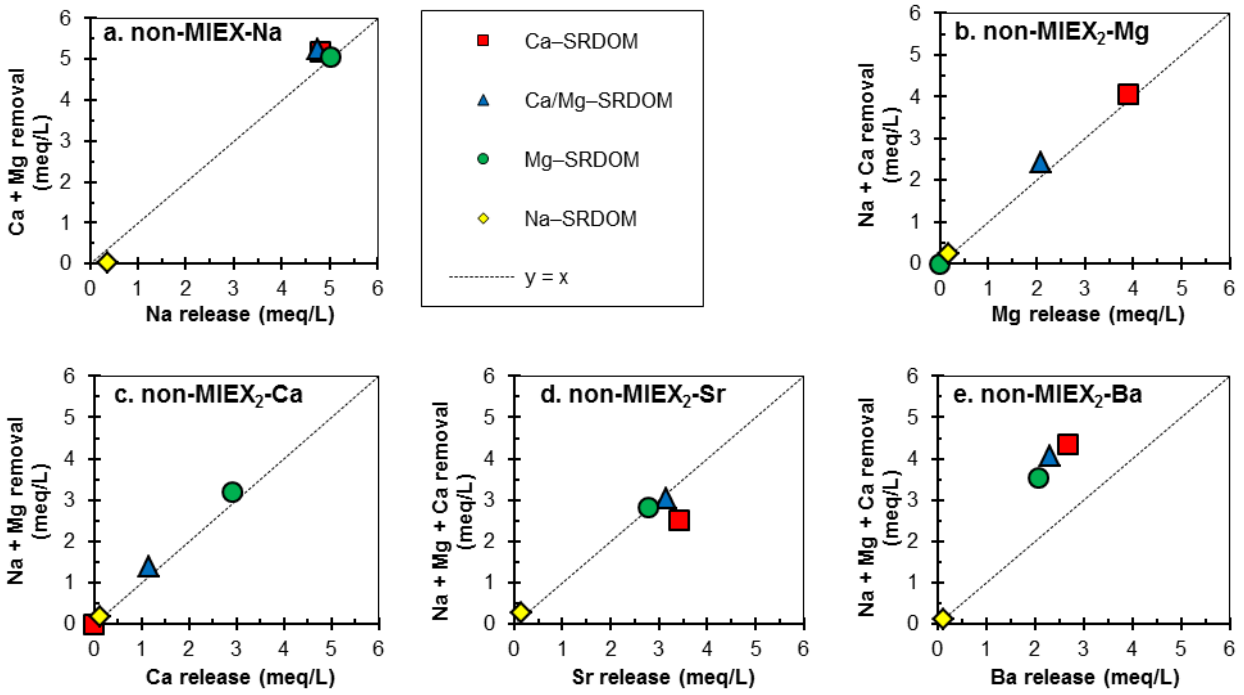

Figure A-3. Cation exchange stoichiometry for Na-, Mg-, Ca-, Sr-, and Ba-forms of non-MIEX resin under varying conditions of metal cations and SRDOM in solution.

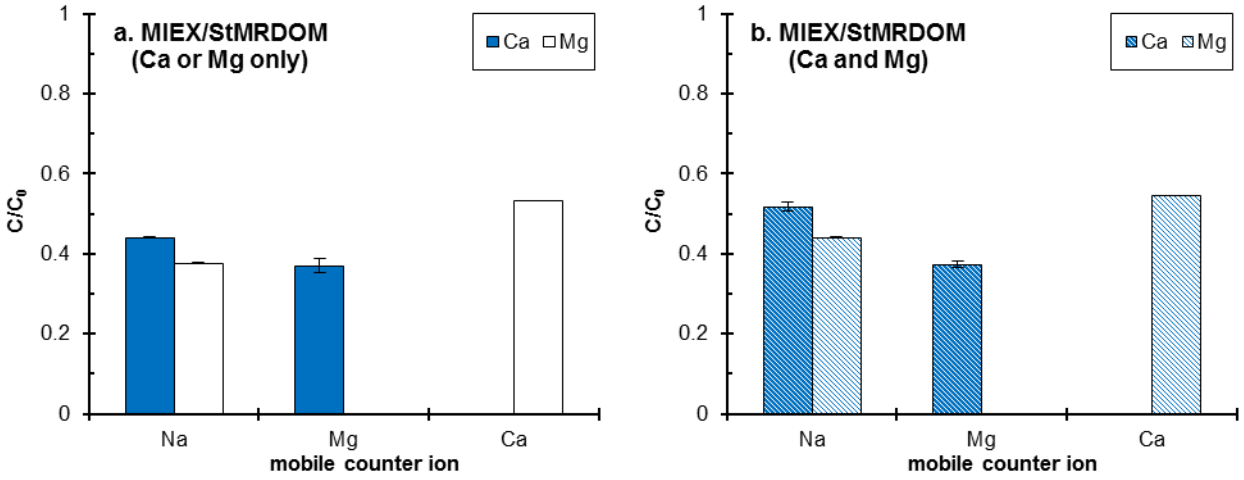

Figure A-4. Calcium and magnesium removal for Na-, Mg-, Ca-, Sr-, and Ba-forms of MIEX resin in the absence/presence of StMRDOM. A-C) Ca^{2+} or Mg^{2+} in aqueous phase (~2.5 mmol/L). D-E) Both Ca^{2+} (~1.25 mmol/L) and Mg^{2+} (~1.25 mmol/L) in aqueous phase. Error bars show the standard error for duplicate samples. Magnesium increase from Mg-form resin and calcium increase from Ca-form resin not shown.

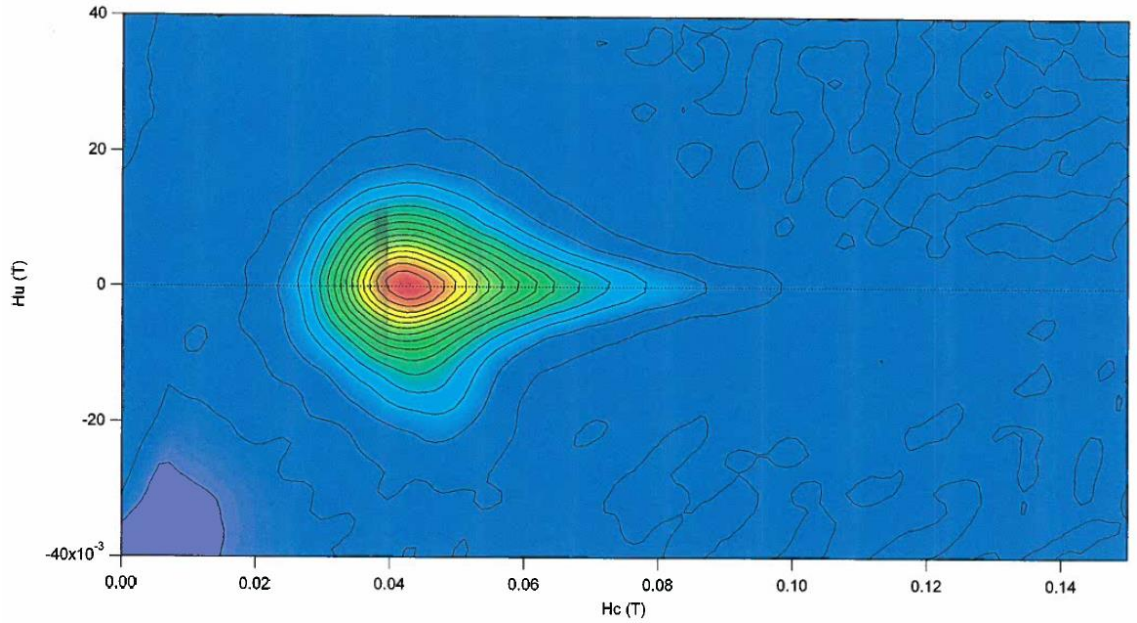

Figure A-5. FORC diagram for MIEX-Ca resin.

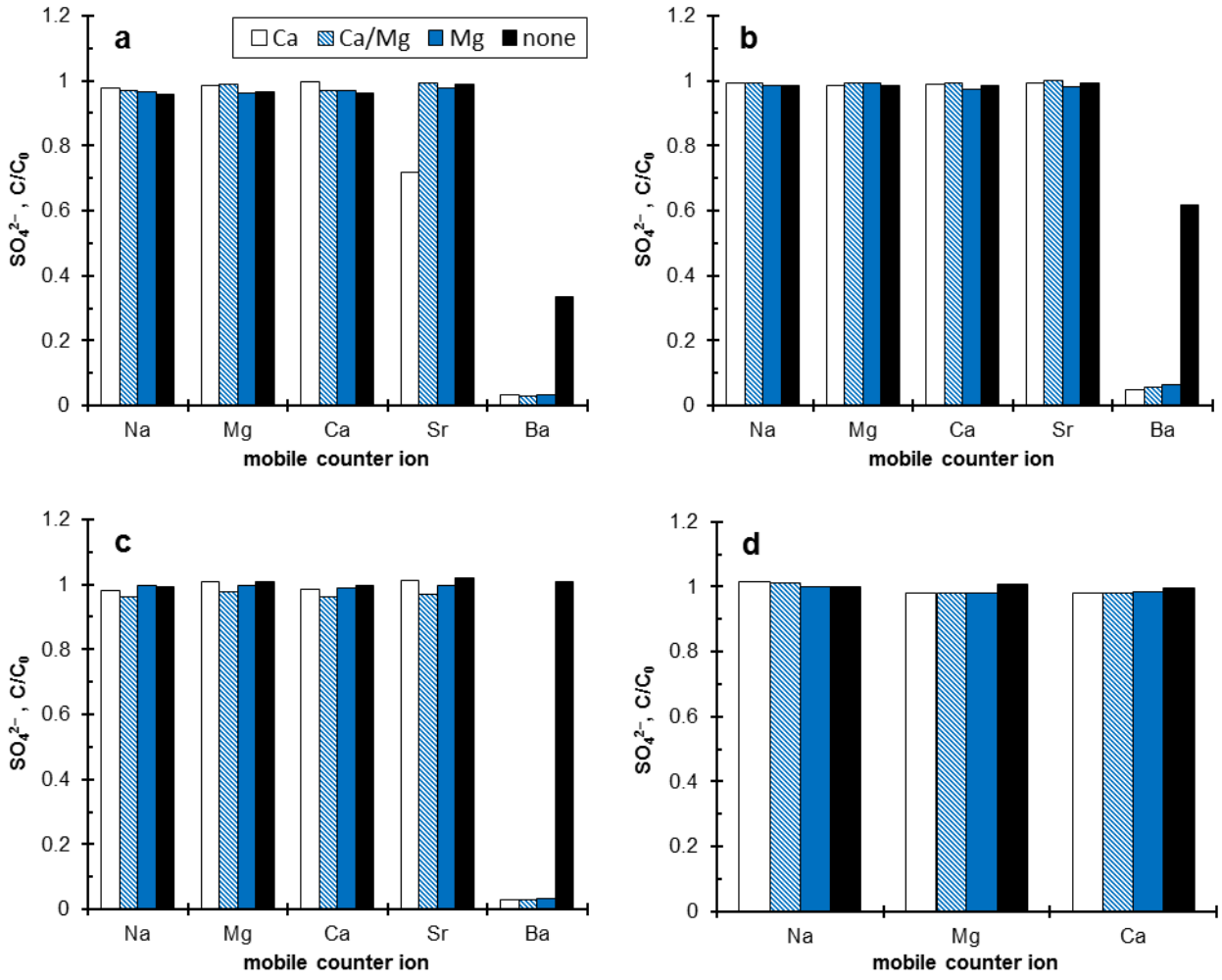

Figure A-6. Normalized sulfate concentrations following Na-, Mg-, Ca-, Sr-, and Ba-form cation exchange. A) MIEX resin/no DOM. B) MIEX resin/SRDOM. C) Non-MIEX resin/SRDOM. D) MIEX resin/StMRDOM.

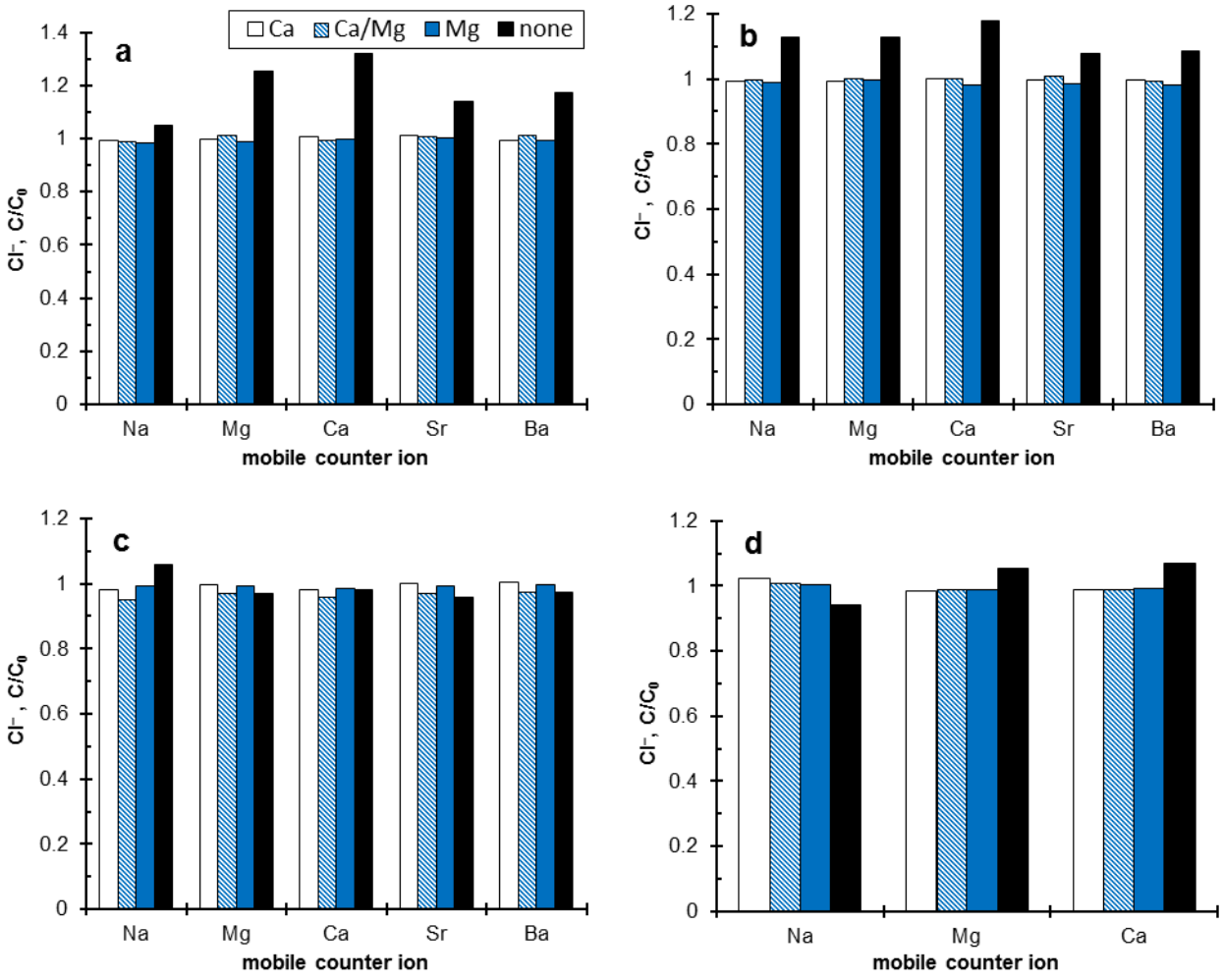

Figure A-7. Normalized chloride concentrations following Na-, Mg-, Ca-, Sr-, and Ba-form cation exchange. A) MIEX resin/no DOM. B) MIEX resin/SRDOM. C) Non-MIEX resin/SRDOM. D) MIEX resin/StMRDOM.

APPENDIX B
SUPPLEMENTARY INFORMATION FOR CHAPTER 3

Error bar calculations

All experiments were conducted in triplicate; therefore error bars for Figures 3-2 and 3-3 were calculated as one standard deviation from the mean. The data displayed in those figures are a function of the average initial concentration minus the average final concentration after ion exchange. Section 2.5.5.2 of The Engineering Statistics Handbook reports appropriate calculations for the standard deviation of the function of two variables [83]. The appropriate equation used for this data set is as follows:

$$Y = A\bar{X} + B\bar{Z} \quad \text{Eq. B-1}$$

Where A=1, B=-1, $\bar{X}$=initial concentration before ion exchange (control samples), and $\bar{Z}$=concentration after ion exchange.

$$St.\,Deviation\ of\ Y = \frac{1}{\sqrt{N}}\sqrt{A^2S_x^2 + B^2S_z^2 + 2ABS_{xz}^2} \quad \text{Eq. B-2}$$

Where N=3 (triplicate samples), A and B are previously defined, S_x^2=variance of control samples, S_z^2=variance of experimental samples, and S_{xz}^2=covariance of the control and the experimental samples (calculated in Excel).

Separation Factor calculations

Separation factors were calculated according to the following equation:

$$\alpha_{A/B} = \frac{q_B C_A}{C_B q_A} \quad \text{Eq. B-3}$$

where A=presaturant ion initially on the ion exchange resin, B=ion removed from solution during ion exchange treatment, *q*=resin phase concentration at equilibrium (meq/g), and *C* is aqueous phase concentration at equilibrium (meq/L). A sample

calculation for the separation factor for Na^+/Ca^{2+} (cation exchange) during the combined ion exchange experiment with the calcium hardness water is as follows:

$$\alpha_{A/B} = \frac{q_B C_A}{C_B q_A} \quad \text{Eq. B-4}$$

$$\alpha_{Na/Ca} = \frac{q_{Ca} C_{Na}}{C_{Ca} q_{Na}} \quad \text{Eq. B-5}$$

C_{Na} and C_{Ca} are aqueous phase concentrations at equilibrium. After the calcium hardness water underwent combined ion exchange for 2 days, the final sodium concentration was 10.795 meq/L and the final calcium concentration was 0.119 meq/L. The amount of calcium sorbed onto the resin is the difference between the initial concentration and the final concentration, accounting for mass of resin and volume of solution. In general,

$$q = \frac{V}{m}(|C_f - C_i|) \quad \text{Eq. B-6}$$

The volume of sample during combined ion exchange was 0.1L and the mass of cation exchange resin (Amberlite 200C) used was 0.17856g. The final concentration of calcium in solution was 0.119 meq/L and the initial concentration was 4.969 meq/L. Therefore, q_{Ca}=2.716 meq/g. The amount of sodium sorbed onto the resin is the initial capacity of the resin minus the sodium released to solution (again accounting for the mass of resin and volume of sample). The capacity of the resin is 1.7 meq/mL (from manufacturer) and the density of the resin was experimentally determined to be 0.4464 g/mL (average of triplicate analysis). Therefore the initial capacity of the resin is (1.7 meq/mL)/(0.4464 g/mL) = 3.81 meq/g. Following equation S6, q_{Na}=3.81 meq/g – (0.1L/0.17856g)*(10.795meq/L – 5.972 meq/L) = 1.107 meq/g. Plugging all variables into equation S5, yields the following:

$$\alpha_{Na/Ca} = \frac{q_{Ca} C_{Na}}{C_{Ca} q_{Na}} = \frac{2.716 * 10.795}{0.119 * 1.107} = 222.565$$

Adhering to 2 significant figures, we arrive at a separation factor of 220 for the preference of calcium to sodium during combined ion exchange in the calcium hardness water.

APPENDIX C
SUPPLEMENTARY INFORMATION FOR CHAPTER 4

pH Water Quality Data

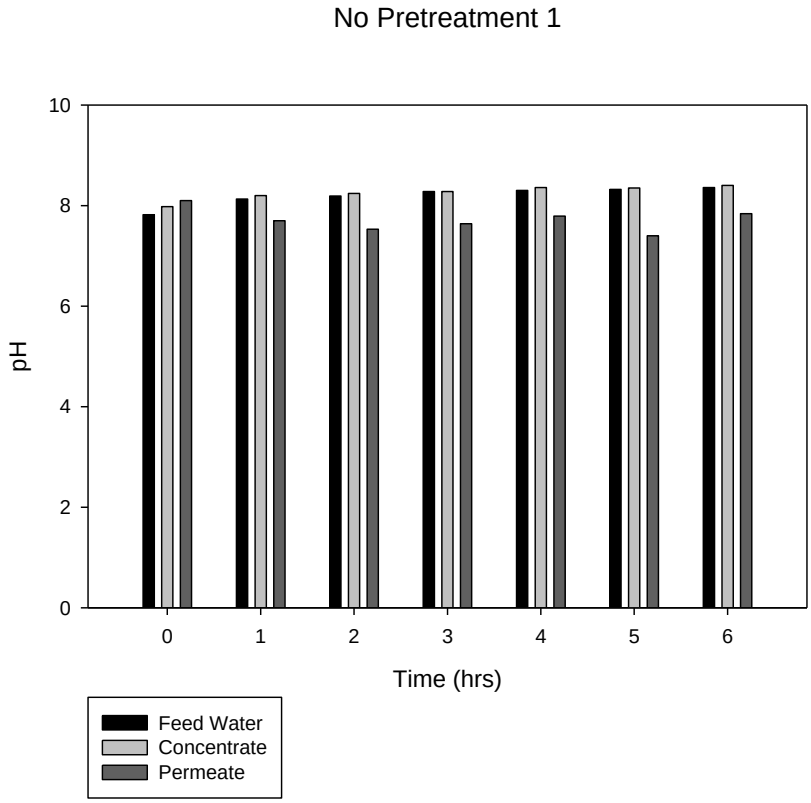

Figure C-1. pH for NaCl spiked Cedar Key water with no pretreatment (first sample) before RO filtration. A) Feed Water. B) Concentrate. C) Permeate.

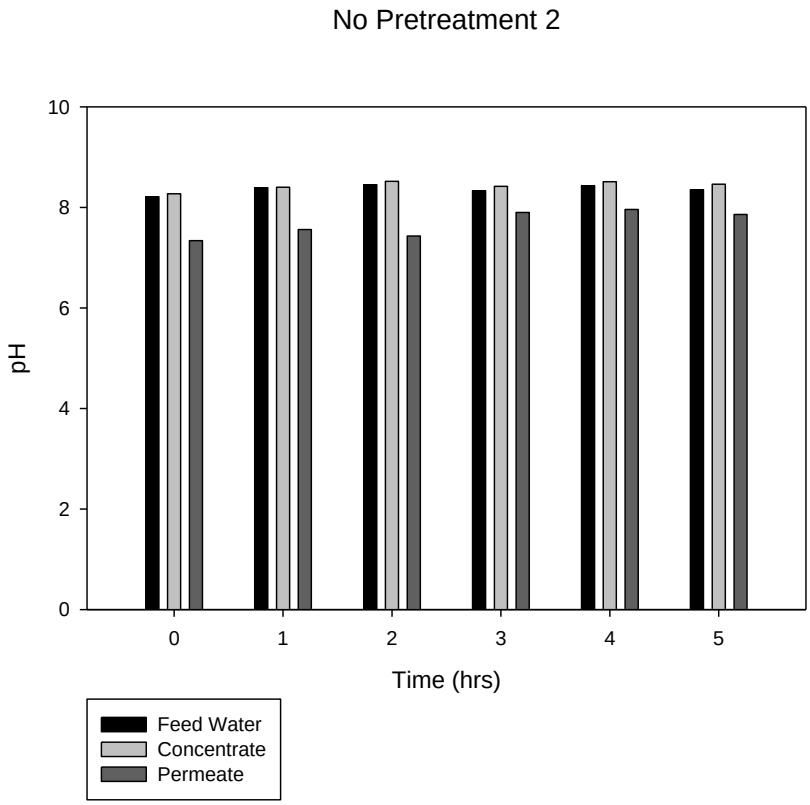

Figure C-2. pH for NaCl spiked Cedar Key water with no pretreatment (second sample) before RO filtration. A) Feed Water. B) Concentrate. C) Permeate.

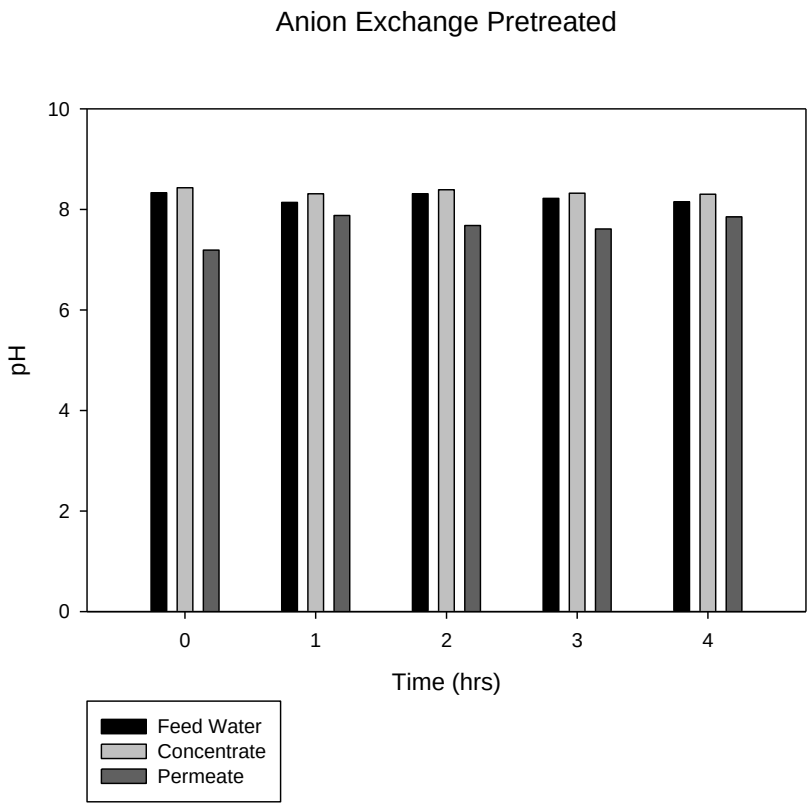

Figure C-3. pH for NaCl spiked Cedar Key water with anion exchange pretreatment before RO filtration. A) Feed Water. B) Concentrate. C) Permeate.

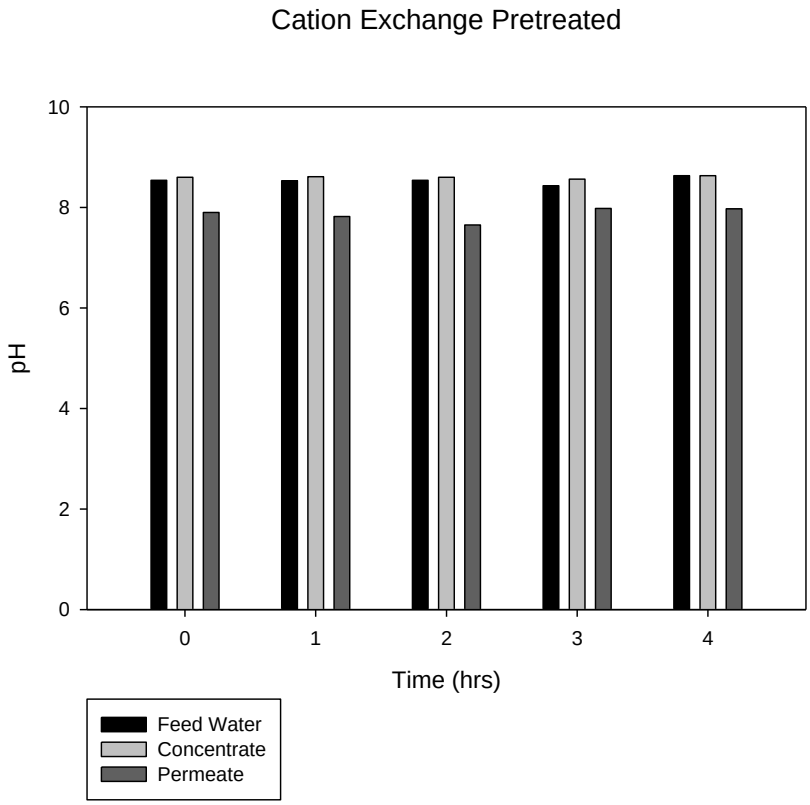

Figure C-4. pH for NaCl spiked Cedar Key water with cation exchange pretreatment before RO filtration. A) Feed Water. B) Concentrate. C) Permeate.

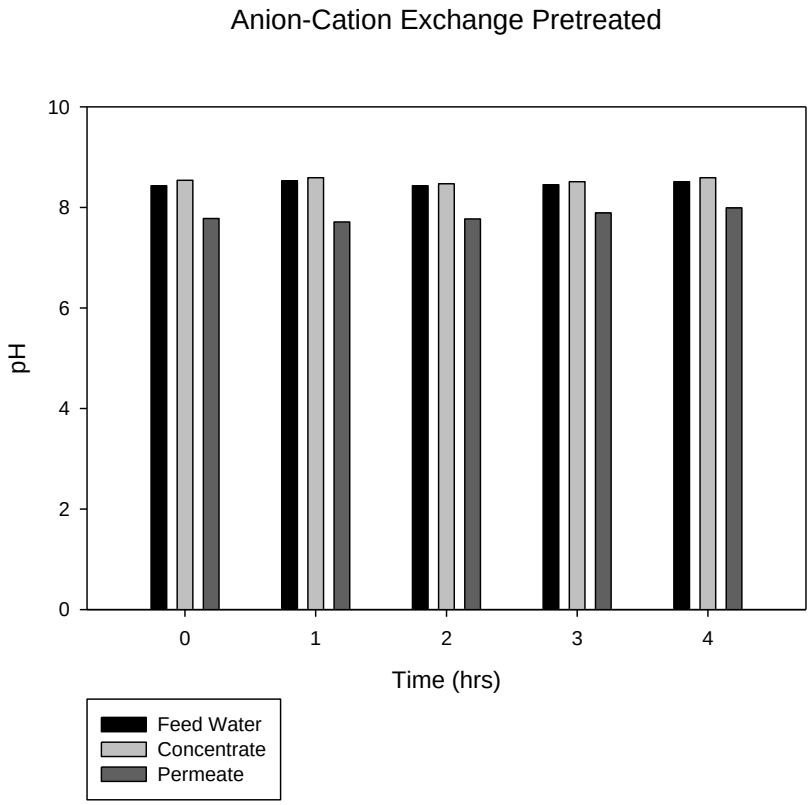

Figure C-5. pH for NaCl spiked Cedar Key water with anion and cation exchange pretreatment (combined ion exchange) before RO filtration. A) Feed Water. B) Concentrate. C) Permeate.

LIST OF REFERENCES

1. Barnett, T. P.; Pierce, D. W.; Hidalgo, H. G.; Bonfils, C.; Santer, B. D.; Das, T.; Bala, G.; Wood, A. W.; Nozawa, T.; Mirin, A. A.; Cayan, D. R.; Dettinger, M. D., Human-induced changes in the hydrology of the western United States. *Science* **2008,** *319*, (5866), 1080-1083.

2. Wei, X.; Wang, Z.; Fan, F.; Wang, J.; Wang, S., Advanced treatment of a complex pharmaceutical wastewater by nanofiltration: Membrane foulant identification and cleaning. *Desalination 251*, (1-3), 167-175.

3. Delpla, I.; Jung, A. V.; Baures, E.; Clement, M.; Thomas, O., Impacts of climate change on surface water quality in relation to drinking water production. *Environment International* **2009,** *35*, (8), 1225-1233.

4. Zimmerman, J. B.; Mihelcic, J. R.; Smith, J., Global stressors on water quality and quantity. *Environmental Science & Technology* **2008,** *42*, (12), 4247-4254.

5. Bonte, M.; Zwolsman, J. J. G., Climate change induced salinisation of artificial lakes in the Netherlands and consequences for drinking water production. *Water Research* **2010,** *44*, (15), 4411-4424.

6. Haaland, S.; Hongve, D.; Laudon, H.; Riise, G.; Vogt, R. D., Quantifying the Drivers of the Increasing Colored Organic Matter in Boreal Surface Waters. *Environmental Science & Technology* **2010,** *44*, (8), 2975-2980.

7. Van der Bruggen, B.; Lejon, L.; Vandecasteele, C., Reuse, treatment, and discharge of the concentrate of pressure-driven membrane processes. *Environmental Science & Technology* **2003,** *37*, (17), 3733-3738.

8. Al-Amoudi, A. S., Factors affecting natural organic matter (NOM) and scaling fouling in NF membranes: A review. *Desalination* **2010,** *259*, (1-3), 1-10.

9. Rahardianto, A.; Gao, J. B.; Gabelich, C. J.; Williams, M. D.; Cohen, Y., High recovery membrane desalting of low-salinity brackish water: Integration of accelerated precipitation softening with membrane RO. *Journal of Membrane Science* **2007,** *289*, (1-2), 123-137.

10. Wang, Y. N.; Tang, C. Y., Nanofiltration Membrane Fouling by Oppositely Charged Macromolecules: Investigation on Flux Behavior, Foulant Mass Deposition, and Solute Rejection. *Environmental Science & Technology 45*, (20), 8941-8947.

11. Jin, X.; Huang, X. F.; Hoek, E. M. V., Role of Specific Ion Interactions in Seawater RO Membrane Fouling by Alginic Acid. *Environmental Science & Technology* **2009,** *43*, (10), 3580-3587.

12. Ahn, W. Y.; Kalinichev, A. G.; Clark, M. M., Effects of background cations on the fouling of polyethersulfone membranes by natural organic matter: Experimental and molecular modeling study. *Journal of Membrane Science* **2008,** *309*, (1-2), 128-140.

13. Yoon, S. H.; Lee, C. H.; Kim, K. J.; Fane, A. G., Effect of calcium ion on the fouling of nanofilter by humic acid in drinking water production. *Water Research* **1998,** *32*, (7), 2180-2186.

14. Li, Q. L.; Elimelech, M., Organic fouling and chemical cleaning of nanofiltration membranes: Measurements and mechanisms. *Environmental Science & Technology* **2004,** *38*, (17), 4683-4693.

15. Lin, N. H.; Shih, W. Y.; Lyster, E.; Cohen, Y., Crystallization of calcium sulfate on polymeric surfaces. *Journal of Colloid and Interface Science* **2011,** *356*, (2), 790-797.

16. Lin, C. J.; Shirazi, S.; Rao, P.; Agarwal, S., Effects of operational parameters on cake formation of CaSO4 in nanofiltration. *Water Research* **2006,** *40*, (4), 806-816.

17. Her, N.; Amy, G.; Plottu-Pecheux, A.; Yoon, Y., Identification of nanofiltration membrane foulants. *Water Research* **2007,** *41*, (17), 3936-3947.

18. Huang, H.; Schwab, K.; Jacangelo, J. G., Pretreatment for Low Pressure Membranes in Water Treatment: A Review. *Environmental Science & Technology* **2009,** *43*, (9), 3011-3019.

19. Kim, M. M.; Au, J.; Rahardianto, A.; Glater, J.; Cohen, Y.; Gerringer, F. W.; Gabelich, C. J., Impact of Conventional Water Treatment Coagulants on Mineral Scaling in RO Desalting of Brackish Water. *Industrial & Engineering Chemistry Research* **2009,** *48*, (6), 3126-3135.

20. Cornelissen, E. R.; Beerendonk, E. F.; Nederlof, M. N.; van der Hoek, J. P.; Wessels, L. P., Fluidized ion exchange (FIX) to control NOM fouling in ultrafiltration. *Desalination* **2009,** *236*, (1-3), 334-341.

21. Verliefde, A. R. D.; Cornelissen, E. R.; Heijman, S. G. J.; Petrinic, I.; Luxbacher, T.; Amy, G. L.; Van der Bruggen, B.; van Dijk, J. C., Influence of membrane fouling by (pretreated) surface water on rejection of pharmaceutically active compounds (PhACs) by nanofiltration membranes. *Journal of Membrane Science* **2009,** *330*, (1-2), 90-103.

22. Abrahamse, A. J.; Lipreau, C.; Li, S.; Heijman, S. G. J., Removal of divalent cations reduces fouling of ultrafiltration membranes. *Journal of Membrane Science* **2008,** *323*, (1), 153-158.

23. Cornelissen, E. R.; Chasseriaud, D.; Siegers, W. G.; Beerendonk, E. F.; van der Kooij, D., Effect of anionic fluidized ion exchange (FIX) pre-treatment on nanofiltration (NF) membrane fouling. *Water Research* **2010,** *44*, (10), 3283-3293.

24. Heijman, S. G. J.; Guo, H.; Li, S.; van Dijk, J. C.; Wessels, L. P., Zero liquid discharge: Heading for 99% recovery in nanofiltration and reverse osmosis. *Desalination* **2009,** *236*, (1-3), 357-362.

25. Apell, J. N.; Boyer, T. H., Combined ion exchange treatment for removal of dissolved organic matter and hardness. *Water Research* **2010,** *44*, (8), 2419-2430.

26. Boyer, T. H.; Miller, C. T.; Singer, P. C., Advances in Modeling Completely Mixed Flow Reactors for Ion Exchange. *Journal of Environmental Engineering-Asce* **2010,** *136*, (10), 1128-1138.

27. Leenheer, J. A.; Brown, G. K.; MacCarthy, P.; Cabaniss, S. E., Models of metal binding structures in fulvic acid from the Suwannee River, Georgia. *Environmental Science & Technology* **1998,** *32*, (16), 2410-2416.

28. Bose, P.; Reckhow, D. A., Modeling pH and ionic strength effects on proton and calcium complexation of fulvic acid: A tool for drinking water-NOM studies. *Environmental Science & Technology* **1997,** *31*, (3), 765-770.

29. Kalinichev, A. G.; Kirkpatrick, R. J., Molecular dynamics simulation of cationic complexation with natural organic matter. *European Journal of Soil Science* **2007,** *58*, (4), 909-917.

30. Milne, C. J.; Kinniburgh, D. G.; Van Riemsdijk, W. H.; Tipping, E., Generic NICA-Donnan model parameters for metal-ion binding by humic substances. *Environmental Science & Technology* **2003,** *37*, (5), 958-971.

31. Dong, W. M.; Brooks, S. C., Determination of the formation constants of ternary complexes of uranyl and carbonate with alkaline earth metals (Mg2+, Ca2+, Sr2+, and Ba2+) using anion exchange method. *Environmental Science & Technology* **2006,** *40*, (15), 4689-4695.

32. Boyer, T. H.; Singer, P. C., Stoichiometry of removal of natural organic matter by ion exchange. *Environmental Science & Technology* **2008,** *42*, (2), 608-613.

33. Boyer, T. H.; Singer, P. C.; Aiken, G. R., Removal of dissolved organic matter by anion exchange: Effect of dissolved organic matter properties. *Environmental Science & Technology* **2008,** *42*, (19), 7431-7437.

34. Cornelissen, E. R.; Moreau, N.; Siegers, W. G.; Abrahamse, A. J.; Rietueld, L. C.; Grefte, A.; Dignum, M.; Amy, G.; Wessels, L. P., Selection of anionic exchange resins for removal of natural organic matter (NOM) fractions. *Water Research* **2008,** *42*, (1-2), 413-423.

35. Drikas, M.; Dixon, M.; Morran, J., Long term case study of MIEX pre-treatment in drinking water; understanding NOM removal. *Water Research* **2011,** *45*, (4), 1539-1548.

36. Davis, W. M.; Erickson, C. L.; Johnston, C. T.; Delfino, J. J.; Porter, J. E., Quantitative Fourier Transform Infrared spectroscopic investigation of humic substance functional group composition. *Chemosphere* **1999,** *38*, (12), 2913-2928.

37. Walker, K. M.; Boyer, T. H., Long-term performance of bicarbonate-form anion exchange: Removal of dissolved organic matter and bromide from the St. Johns River, FL, USA. *Water Research* **2011,** *45*, (9), 2875-2886.

38. Rokicki, C. A.; Boyer, T. H., Bicarbonate-form anion exchange: Affinity, regeneration, and stoichiometry. *Water Research* **2011,** *45*, (3), 1329-1337.

39. American Water Works, A.; Edzwald, J. K., *Water quality & treatment a handbook on drinking water*. McGraw-Hill: New York, 2011.

40. Helfferich, F. G., *Ion Exchange*. McGraw-Hill: 1962.

41. Ritchie, J. D.; Perdue, E. M., Proton-binding study of standard and reference fulvic acids, humic acids, and natural organic matter. *Geochimica Et Cosmochimica Acta* **2003,** *67*, (1), 85-96.

42. Li, P.; Sengupta, A. K., Genesis of selectivity and reversibility for sorption of synthetic aromatic anions onto polymeric sorbents. *Environmental Science & Technology* **1998,** *32*, (23), 3756-3766.

43. Lin, Y. P.; Singer, P. C.; Aiken, G. R., Inhibition of calcite precipitation by natural organic material: Kinetics, mechanism, and thermodynamics. *Environmental Science & Technology* **2005,** *39*, (17), 6420-6428.

44. Weishaar, J. L.; Aiken, G. R.; Bergamaschi, B. A.; Fram, M. S.; Fujii, R.; Mopper, K., Evaluation of specific ultraviolet absorbance as an indicator of the chemical composition and reactivity of dissolved organic carbon. *Environmental Science & Technology* **2003,** *37*, (20), 4702-4708.

45. Singer, P. C.; Boyer, T.; Holmquist, A.; Morran, J.; Bourke, M., Integrated analysis of NOM removal by magnetic ion exchange. *Journal American Water Works Association* **2009,** *101*, (1), 65-+.

46. Hong, R. Y.; Feng, B.; Cai, X.; Liu, G.; Li, H. Z.; Ding, J.; Zheng, Y.; Wei, D. G., Double-Miniemulsion Preparation of Fe3O4/Poly(methyl methacrylate) Magnetic Latex. *Journal of Applied Polymer Science* **2009,** *112*, (1), 89-98.

47. Lee, Y.; Rho, J.; Jung, B., Preparation of magnetic ion-exchange resins by the suspension polymerization of styrene with magnetite. *Journal of Applied Polymer Science* **2003,** *89*, (8), 2058-2067.

48. Kosmulski, M., Compilation of PZC and IEP of sparingly soluble metal oxides and hydroxides from literature. *Advances in Colloid and Interface Science* **2009,** *152*, (1-2), 14-25.

49. Singh, B. K.; Jain, A.; Kumar, S.; Tomar, B. S.; Tomar, R.; Manchanda, V. K.; Ramanathan, S., Role of magnetite and humic acid in radionuclide migration in the environment. *Journal of Contaminant Hydrology* **2009,** *106*, (3-4), 144-149.

50. Illes, E.; Tombacz, E., The effect of humic acid adsorption on pH-dependent surface charging and aggregation of magnetite nanoparticles. *Journal of Colloid and Interface Science* **2006,** *295*, (1), 115-123.

51. Tang, S. C. N.; Wang, P.; Yin, K.; Lo, I. M. C., Synthesis and Application of Magnetic Hydrogel for Cr(VI) Removal from Contaminated Water. *Environmental Engineering Science* **2010,** *27*, (11), 947-954.

52. Philippova, O.; Barabanova, A.; Molchanov, V.; Khokhlov, A., Magnetic polymer beads: Recent trends and developments in synthetic design and applications. *European Polymer Journal* **2011,** *47*, (4), 542-559.

53. Hsu, S.; Singer, P. C., Application of anion exchange to control NOM interference on lime softening. *Journal American Water Works Association* **2009,** *101*, (6), 85-+.

54. Jin, J.; Zimmerman, A. R., Abiotic interactions of natural dissolved organic matter and carbonate aquifer rock. *Applied Geochemistry* **2010,** *25*, (3), 472-484.

55. McKnight, D. M.; Andrews, E. D.; Spaulding, S. A.; Aiken, G. R., Aquatic fulvic-acids in algal-rich antarctic ponds. *Limnology and Oceanography* **1994,** *39*, (8), 1972-1979.

56. Thurman, M., *Organic Geochemistry of Natural Waters*. Martinus Nijhoff/Dr W. Junk Publishers: 1985.

57. Bolto, B.; Dixon, D.; Eldridge, R.; King, S.; Linge, K., Removal of natural organic matter by ion exchange. *Water Research* **2002,** *36*, (20), 5057-5065.

58. Stumm, W.; Morgan, J. J.; Morgan, J. J. j. a., *Aquatic chemistry : an introduction emphasizing chemical equilibria in natural waters / Werner Stumm, James J. Morgan*. Wiley: New York, 1981.

59. Louis, Y.; Garnier, C.; Lenoble, V.; Omanovic, D.; Mounier, S.; Pizeta, I., Characterisation and modelling of marine dissolved organic matter interactions with major and trace cations. *Marine Environmental Research* **2009,** *67*, (2), 100-107.

60. Boyer, T. H.; Singer, P. C., Bench-scale testing of a magnetic ion exchange resin. for removal of disinfection by-product precursors. *Water Research* **2005,** *39*, (7), 1265-1276.

61. Tan, Y. R.; Kilduff, J. E.; Kitis, M.; Karanfil, T., Dissolved organic matter removal and disinfection byproduct formation control using ion exchange. *Desalination* **2005,** *176*, (1-3), 189-200.

62. Cho, J. W.; Amy, G.; Pellegrino, J.; Yoon, Y. M., Characterization of clean and natural organic matter (NOM) fouled NF and UF membranes, and foulants characterization. *Desalination* **1998,** *118*, (1-3), 101-108.

63. Lee, H.; Amy, G.; Cho, J.; Yoon, Y.; Moon, S.-H.; Kim, I. S., Cleaning strategies for flux recovery of an ultrafiltration membrane fouled by natural organic matter. *Water Research* **2001,** *35*, (14), 3301-3308.

64. Maartens, A.; Swart, P.; Jacobs, E. P., Membrane pretreatment: A method for reducing fouling by natural organic matter. *Journal of Colloid and Interface Science* **2000,** *221*, (2), 137-142.

65. Bolto, B.; Dixon, D.; Eldridge, R., Ion exchange for the removal of natural organic matter. *Reactive & Functional Polymers* **2004,** *60*, 171-182.

66. Bond, T.; Goslan, E. H.; Parsons, S. A.; Jefferson, B., Disinfection by-product formation of natural organic matter surrogates and treatment by coagulation, MIEXÂ® and nanofiltration. *Water Research* **2010,** *44*, (5), 1645-1653.

67. Jarvis, P.; Mergen, M.; Banks, J.; McIntosh, B.; Parsons, S. A.; Jefferson, B., Pilot scale comparison of enhanced coagulation with magnetic resin plus coagulation systems. *Environmental Science & Technology* **2008,** *42*, (4), 1276-1282.

68. Indarawis, K.; Boyer, T. H., Alkaline Earth Metal Cation Exchange: Effect of Mobile Counterion and Dissolved Organic Matter. *Environmental Science & Technology* **2012,** *46*, (8), 4591-4598.

69. Wang, Y.; Sikora, S.; Kim, H.; Dubey, B.; Townsend, T., Mobilization of iron and arsenic from soil by construction and demolition debris landfill leachate. *Waste Management* **2012,** *32*, (5), 925-932.

70. Comstock, S. Physical-Chemical Treatment of Groundwater and Membrane Concentrate to Decrease Membrane Fouling Potential. University of Florida, Gainesville, FL, 2011.

71. Comstock, S. E. H.; Boyer, T. H.; Graf, K. C., Treatment of nanofiltration and reverse osmosis concentrates: Comparison of precipitative softening, coagulation, and anion exchange. *Water Research* **2011,** *45*, (16), 4855-4865.

72. Aniceto, J. P. S.; Cardoso, S. P.; Faria, T. L.; Lito, P. F.; Silva, C. M., Modeling ion exchange equilibrium: Analysis of exchanger phase non-ideality. *Desalination* **2012,** *290*, 43-53.

73. Boyer, T. H.; Miller, C. T.; Singer, P. C., Modeling the removal of dissolved organic carbon by ion exchange in a completely mixed flow reactor. *Water Research* **2008,** *42*, (8-9), 1897-1906.

74. Carmona, M.; De Lucas, A.; Valverde, J. L.; Velasco, B.; Rodriguez, J. F., Combined adsorption and ion exchange equilibrium of phenol on Amberlite IRA-420. *Chemical Engineering Journal* **2006,** *117*, (2), 155-160.

75. Dron, J.; Dodi, A., Comparison of adsorption equilibrium models for the study of CL-, NO3- and SO42- removal from aqueous solutions by an anion exchange resin. *Journal of Hazardous Materials* **2011,** *190*, (1-3), 300-307.

76. Dron, J.; Dodi, A., Thermodynamic Modeling of Cl-, NO3- and SO42- Removal by an Anion Exchange Resin and Comparison with Dubinin-Astakhov Isotherms. *Langmuir* **2011,** *27*, (6), 2625-2633.

77. Klika, Z.; Kraus, L.; Vopalka, D., Cesium uptake from aqueous solutions by bentonite: A comparison of multicomponent sorption with ion-exchange models. *Langmuir* **2007,** *23*, (3), 1227-1233.

78. Plazinski, W.; Rudzinski, W., Binding stoichiometry in sorption of divalent metal ions: A theoretical analysis based on the ion-exchange model. *Journal of Colloid and Interface Science* **2010,** *344*, (1), 165-170.

79. Essington, M. E., *Soil and Water Chemistry: An Integrative Approach*. CRC PressINC: 2004.

80. Indarawis, K.; Boyer, T. H., Superposition of anion and cation exchange for removal of natural water ions. *Separation and Purification Technology* **2013**.

81. Li, Q. L.; Elimelech, M., Revealing the mechanisms of organic fouling and chemical cleaning of nanofiltration membranes. *Abstracts of Papers of the American Chemical Society* **2003,** *226*, 237-ENVR.

82. Shih, W. Y.; Rahardianto, A.; Lee, R. W.; Cohen, Y., Morphometric characterization of calcium sulfate dihydrate (gypsum) scale on reverse osmosis membranes. *Journal of Membrane Science* **2005,** *252*, (1-2), 253-263.

83. NIST/SEMATECH e-Handbook of Statistical Methods. http://www.itl.nist.gov/div898/handbook/

84. Dunlop, D. J., Magnetite - behavior near single-domain threshold. *Science* **1972,** *176*, (4030), 41-&.

85. Dunlop, D. J., Hysteresis properties of magnetite and their dependence on particle-size - a test of pseudo-single-domain remanence models. *Journal of Geophysical Research-Solid Earth and Planets* **1986,** *91*, (B9), 9569-9584.

86. Dunlop, D. J., Theory and application of the Day plot (M-rs/M-s versus H-cr/H-c) 1. Theoretical curves and tests using titanomagnetite data. *Journal of Geophysical Research-Solid Earth* **2002,** *107*, (B3).

87. Mayergoyz, I. D., Mathematical-models of hysteresis. *Ieee Transactions on Magnetics* **1986,** *22*, (5), 603-608.

88. Pike, C. R.; Roberts, A. P.; Verosub, K. L., Characterizing interactions in fine magnetic particle systems using first order reversal curves. *Journal of Applied Physics* **1999,** *85*, (9), 6660-6667.

89. (ATSDR), A. f. T. S. a. D. R., Toxilogical profile for Strontium. In Services, U. S. D. o. H. a. H., Ed. Public Health Service: Atlanta, GA, 2004.

90. (ATSDR), A. f. T. S. a. D. R., Toxilogical profile for Barium. In US Department of Health and Human Services, Public Health Service: Atlanta, GA, 2007.

91. Morel, F. M. M.; Hering, J. G., *Principles and Applications of Aquatic Chemistry*. Wiley: 1993.

BIOGRAPHICAL SKETCH

Katrina Indarawis obtained a BA in mathematics and a BS in statistics from the University of Florida in May 2002. Shortly after, she married her husband, of more than ten years now, and continued her academics with a MS in education (Summer 2004). After briefly teaching at Gainesville High School, she returned to UF for a BS in civil engineering (December 2007). She then had her first daughter (now 5 years old) and worked with Dr. David Mazyck in one of his off-campus labs. After being awarded a Graduate Alumni Fellowship, she returned for her PhD in the fall of 2009 under the advisement of Dr. Treavor Boyer. She had her second daughter (now 3 years old) her first semester of her PhD. She received her PhD from the University of Florida in the summer of 2013.